Cadomia origins: Paired Ediacaran ophiolites from the Iberian Massif, the opening and closure record of peri-Gondwanan basins

Ricardo Arenas[1]*, Christian Vérard[2], Richard Albert[3,4], Esther Rojo-Pérez[1], Sonia Sánchez Martínez[1], Irene Novo-Fernández[1], Diana Moreno-Martín[1], Axel Gerdes[3,4], Antonio Garcia-Casco[5], Rubén Díez Fernández[6]

[1]Departamento de Mineralogía y Petrología and Instituto de Geociencias (UCM, CSIC), Universidad Complutense. Madrid, Spain

[2]Department of Earth Sciences, University of Geneva. Geneva, Switzerland

[3]Institut of Geosciences, Goethe University Frankfurt. Frankfurt am Main, Germany

[4]Frankfurt Isotope and Element Research Center (FIERCE), Goethe University Frankfurt. Frankfurt am Main, Germany

[5]Departamento de Mineralogía y Petrología and Instituto Andaluz de Ciencias de la Tierra (UGR, CSIC), Universidad de Granada. Granada, Spain

[6]Instituto Geológico y Minero de España – CSIC. Salamanca, Spain

*Corresponding author at: Departamento de Mineralogía y Petrología and Instituto de Geociencias (UCM, CSIC), Facultad de Geología, Universidad Complutense de Madrid, José Antonio Novais, no 12, 28040 Madrid, Spain.

E-mail addresses:

rarenas@ucm.es (Ricardo Arenas)

christian.verard@unige.ch (Christian Vérard)

albertroper@em.uni-frankfurt.de (Richard Albert)

e.rojo@ucm.es (Esther Rojo-Pérez)

s.sanchez@geo.ucm.es (Sonia Sánchez Martínez)

inovo@ucm.es (Irene Novo-Fernández)

gerdes@fierce.uni-frankfurt.de (Axel Gerdes)

agcasco@ugr.es (Antonio Garcia-Casco)

r.diez@igme.es (Rubén Díez Fernández)

ORCID

R. Arenas - http://orcid.org/0000-0002-8229-4836

C. Vérard – http://orcid.org/0000-0001-9560-6969

R. Albert - http://orcid.org/0000-0002-0185-8581

E. Rojo-Pérez - http://orcid.org/0000-0001-5780-6417

S. Sánchez Martínez - http://orcid.org/0000-0003-0826-5313

I. Novo-Fernández - http://orcid.org/0000-0002-6722-5525

A. Gerdes - http://orcid.org/0000-0003-3823-2125

A. Garcia-Casco - http://orcid.org/0000-0002-8814-402X

R. Díez Fernández - http://orcid.org/0000-0002-0379-7970

Abstract

The recent discovery of Ediacaran ophiolites in the SW Iberian Massif has made it possible to pinpoint the evolution of the Cadomian basement of Europe. The Calzadilla and Merida ophiolites (gabbroic protoliths dated at c. 600 and 594 Ma, respectively) have geochemical characteristics typical of supra-subduction zone ophiolites. They are interpreted as originating during the initial opening of a fore-arc basin with boninitic magmatism (Calzadilla), followed by the formation of a back-arc basin with arc-tholeiites (Merida). Widening of the back-arc leads to the rifting and drifting of a section of the active continental margin (Cadomia). These oceanic domains initiated a rapid contraction, culminating in the collision of Cadomia with Gondwana (c. 590-540 Ma). The application of a PANALESIS model to this paleogeographic setting confirms the plausibility of Cadomian rifting and the likely opening of broad oceanic domains. It also confirms the final collision of Cadomia with Gondwana, although the synthetic and regional data disagree in the precise chronology of the convergence and collision of Cadomia with the West Africa Craton. This work shows that the evolution of the Cadomian basement is much more complex than traditionally considered.

1. Introduction

The Iberian Massif represents an extensive peri-Gondwanan domain with a relevant position during the final assembly of Pangea, when the Variscan Orogen was formed (Fig. 1). It contains a rather continuous orogenic section that includes the innermost domains of the Variscan Orogen, characterized by the presence of different ophiolites and units affected by high-P metamorphism, and foreland areas located further inland in Gondwana, close to the southern deformation front of the Variscan Orogen (Fig. 1; Arenas et al. 2016a, Díez Fernández et al. 2016, Martínez Catalán et al. 2020). It is therefore an optimal region for investigating the long-term evolution of the palaeo-margin of Gondwana, from the formation of the supercontinent to the final assembly of Pangaea.

Different suture zones marked by ophiolites have been recognised in the Iberian Massif, whose continuity through the basement of Central Europe is sometimes unclear (Fig. 2; Arenas et al. 2021). The closest suture to Avalonia is interpreted as the actual suture related to the closure of the Rheic Ocean, the Palaeozoic ocean located between the Avalonia microcontinent and Gondwana (Nance et al. 2010). Ophiolites associated with this suture have been dated to c. 395 Ma in Cornwall (SW England, Lizard Ophiolite; Clark et al. 1998, Nutman et al. 2001). In the SW Iberian Massif, the Beja-Acebuches Ophiolite occupies the same position, but it is younger (c. 340 Ma; Azor et al. 2008; Fig. 2) and its generation seems related to the opening and accretion of a basin following the closure of the Rheic Ocean (Murphy et al. 2011, Díez Fernández et al. 2016). Another Palaeozoic suture identified in the NW Iberian Massif is located farther within Gondwana (Fig. 2). It is a complex suture defined by several ophiolite units dated at c. 500 Ma (Vila de Cruces Ophiolite; Arenas et al. 2007, Sánchez Martínez et al. 2021) and c. 400 Ma (Careón, Purrido and Moeche ophiolites; Díaz García et al. 1999, Pin et al. 2002, Sánchez Martínez et al., 2011, Arenas et al. 2014a). It has been interpreted as a secondary Variscan suture resulting from the closure of an intra-orogenic peri-Gondwanan basin (c. 400 Ma ophiolites, Arenas et al. 2014b) that opened within transitional continental crustal domains (c. 500 Ma ophiolite; Díez Fernández et al. 2016). Ophiolitic units dated at c. 400 Ma are also common in the

Bohemian Massif (Wojtulek et al. 2022). These are the most widely distributed ophiolites in the Variscan Orogen (Kroner and Romer 2013). Finally, the SW Iberian Massif contains another complex suture of Ediacaran age (Fig. 2), defined by the presence of at least two ophiolites dated at c. 600 Ma (Calzadilla and Mérida ophiolites; Arenas et al. 2018, In press, Díez Fernández et al. 2019, 2022). In the vicinity of Iberia, in the Anti Atlas of Morocco, still another older suture zone is dated at c. 750-700 Ma (Bou Azzer Ophiolite; Fig. 2; El Hadi et al 2010, Triantafyllou et al. 2018, Hodel et al 2020, Pujol-Solà et al 2021). Given the ages considered, this suture must be related to the Pan-African dynamics that caused the assembly of the Gondwana supercontinent (Arenas et al. 2021, Vérard 2021).

The presence of Ediacaran ophiolites in the Iberian Massif has only been recently recognized. These ophiolites have not been described so far in other regions of the Variscan Orogen, offering the possibility to investigate the dynamics or orogenic activity of the Gondwana palaeo-margin during the transition between the Ediacaran and the Early Cambrian. These dynamics are referred to as Pan-African orogeny in Africa and Cadomian orogeny in Europe (D`Lemos et al. 1990; Quesada 1990; Liègeois et al. 1994; Von Raumer et al. 2015), where have long remained poorly known due to the involvement of this margin in the final assembly of Pangea, when it represented the Cadomian basement of the Variscan Orogen (Eguíluz et al. 2000) and it was variably deformed during Devonian and Carboniferous times. Interpreting the origin of these ophiolites needs of the carefully analysis of the dynamic setting associated with the development of subduction in the peri-Gondwanan arc system during this period, as well as the possible generation of fore-arc and back-arc basins and the extent of the oceanic domains involved. The characteristics of the ophiolites and the dynamic environments where they may have been generated, can also be discussed based on the predictions of synthetic geodynamics models developed for this period (PANALESIS models, Vérard 2021). This paper presents a review of the currently known data for the Ediacaran ophiolites of the SW Iberian Massif, focusing on the comparison with related terranes, their tectonothermal evolution, lithological, geochemical, isotopic and geochronological characteristics. This dataset is used to discuss the dynamics and possible palaeogeographic evolution of the Ediacaran basement of Europa (Cadomia), both from a regional perspective and in terms of theoretical plate tectonic models. The origin of Cadomia has long been enigmatic, since it has not been possible to clearly recognize its geodynamic setting and evolution. That the Cadomian Orogeny is related to the convergence and interaction of very large continental masses has been generally dismissed. Instead, the Ediacaran dynamics of the African margin of Gondwana has been considered related to the building and dismantling of a long-lived volcanic arc along this margin (Pereira et al. 2006; Linnemann et al. 2008, 2014). In order to determine the identity and chronology of the oceanic domains participating in the evolution of Cadomia, it is essential to trace ophiolitic units generated in both fore-arc and back-arc domains or in the peri-Gondwanan ocean itself. Ophiolite recognition in the field is always challenging and must be supplemented with additional analytical data derived from geochronology, geochemistry and tectonothermal modelling. On the other hand, the results of this work allow us to present a new scenario for the Cadomian Orogeny, where the interaction of Gondwana with lithospheric elements other than the peri-continental volcanic arcs seem to play a significant role.

2. Geological setting

The overall structure of the Variscan Orogen is defined by two main domains. They consist of regions of autochthonous or parautochthonous nature, over which large allochthonous complexes were thrusted, consisting of thick piles of terranes of different nature, both continental and oceanic (Figs. 1 and 3; Arenas et al. 2016a, Díez Fernández et al. 2016, Martínez Catalán et al. 2020, Schulmann et al. 2022). These complexes contain ophiolites of different ages, as described in the previous section, and units affected by several Variscan high pressure (high-P) metamorphic events, the main ones dated at c. 390 Ma and c. 370 Ma (Novo-Fernández et al. In press, and references therein). In the SW Iberian Massif, the Ossa-Morena Complex represents the main allochthonous domain. It is constituted by two assemblages of different nature, an Upper Allochthonous Terrane overlying a Basal Allochthonous Terrane with high-P Variscan metamorphism (Badajoz-

Cordoba Unit or Central Unit), that in turn overrides an Autochthonous Domain (Fig. 3; Díez Fernández and Arenas, 2015). The Upper Allochthonous Terrane is composite, with units of very different nature, dating back to the Carboniferous. Its lower units define a thick lithological stack consisting of Ediacaran and Cambrian age assemblages.

In the Upper Allochthon of the Ossa-Morena Complex, the Ediacaran series represent essentially a section of a peri-Gondwanan magmatic arc, whose record can be traced up to the Early Cambrian. However, it is not a single terrane, as these series include at least two ophiolites of different nature (Calzadilla and Mérida ophiolites; Fig. 3). The magmatic arc contains a thick, mainly siliciclastic, sequence known as the Serie Negra Group (Carvalhosa 1965, Eguiluz 1988), which estimated age ranges from c. 600 Ma to c. 540 Ma for its lower and upper levels (Montemolín and Tentudía formations, respectively; Schäfer et al. 1993, Linnemann et al. 2008, Pereira 2015). This series is intruded by a great diversity of igneous rocks, including gabbroic, tonalitic and granite types, whose age spans almost the entire chronology estimated for the Serie Negra (Rojo-Pérez et al. 2022). The igneous rocks document a long dynamic evolution of the magmatic arc, which is related to a variation in the subduction angle, the amount of subduction-erosion and the involvement of the mantle wedge (Rojo-Pérez et al. 2022). The main episode of deformation and metamorphism affecting the Serie Negra Group has been dated in the northern Ossa-Morena Complex at c. 550-560 Ma (^{40}Ar-^{39}Ar; Blatrix and Burg 1981, Dallmeyer and Quesada 1992).

The Serie Negra Group is unconformably overlain by the Malcocinado Formation (Fricke 1941), mainly composed of andesitic tuffs and massive andesites, with thick levels of polygenic conglomerates at the top and bottom of the formation. This series is less deformed than the Serie Negra Group, and always shows low grade metamorphism. The predominant andesitic composition of the lavas of the Malcocinado Formation, dated at c. 534 Ma (Sarrionandia et al 2020, Rojo-Pérez et al. In press), suggests a mature stage of the peri-Gondwanan arc. Above the Malcocinado Formation, the Torreárboles Formation (Liñán 1984) unconformably overlain the Serie Negra Group and the Malcocinado Formation. This series consists of fluvial to shallow marine shelf deposits of Earliest Cambrian age that reflect a new episode of collapse of the magmatic arc and the onset of a long lasting extensional stage (Middle Cambrian - Early Ordovician) accompanied by alkaline magmatism (Sánchez García et al. 2013).

3. Cadomian ophiolites in SW Iberia

They are represented by the Calzadilla Ophiolite and the Mérida Ophiolite, both recently described (Arenas et al. 2018, In press, Díez Fernández et al. 2019, 2022). These ophiolites were previously interpreted as intrusive massifs formed in relation to the peri-Gondwanan Ediacaran magmatic arc (Gonzalo 1987, Bandrés 2001, Bandrés et al. 2004). The Calzadilla Ophiolite appears to the South in the Ossa Morena Complex, while the Merida Ophiolite is located in a more northerly position (Fig. 3). Considering that in the Ossa Morena Complex the Variscan reworking of the Upper Allochthon is low, these locations are considered an indication of the original position of these units in the active palaeo-margin of northern Gondwana, whose Ediacaran evolution was conditioned by the existence of a subduction zone dipping towards the continent. The characteristics of this subduction zone would have conditioned the dynamics of the margin, the magmatic arc activity and the eventual opening of fore-arc and back-arc basins.

3.1. Calzadilla Ophiolite

3.1.1. Regional setting, lithologies and geochronology

The Calzadilla Ophiolite crops out in a broad antiform beneath the Malcocinado Formation, which rests unconformably over the mafic and ultramafic lithologies and shows low deformation and metamorphism (Díez Fernández et al. 2019). The ophiolite is emplaced by thrusting on the metasedimentary rocks of the Serie Negra. These structural relationships indicate that the ophiolite was obducted onto the Ediacaran siliciclastic series from the peri-Gondwanan magmatic arc. The Calzadilla Ophiolite is composed of a main lower slice and some upper slices that define a tectonic sequence imbricated with the Montemolín Formation (Fig. 4; Arenas et al. 2018, Díez Fernández et al. 2019). The lower slice is c. 1200 m thick and consists of a basal section of ultramafic rocks (serpentinites, pyroxenites and hornblendites) and a thin uppermost layer of medium-coarse grained metagabbros. Diabase dykes and scarce intrusive bodies of felsic rocks of tonalitic compositions and pegmatoid gabbros intrude the ultramafic section of the ophiolite. Podiform chromitite bodies within this mantle section can reach 1-2 m in thickness and about 10 m in length. Chromite shows Al-rich compositions typical of the mantle-crust transition zone (Moho region) of supra-subduction zone ophiolites (Merinero et al. 2013, 2014). The upper imbricate is c. 1500 m thick and contains strongly sheared serpentinites alternating with levels of sliciclastic rocks.

The metagabbros of the lower slice represent a fragment of the crustal section of the ophiolite. They show moderate deformation, with foliation development under metamorphic conditions typical of the low-T part of the amphibolite facies. However, the felsic rocks and pegmatoid gabbros included in the ultramafic rocks show evidence of high-T deformation and local partial melting associated with intense shearing. This tectonothermal evolution prior to serpentinization contrasts with that of the crustal gabbros. It was generated within the mantle before the emplacement of the ophiolite above the Serie Negra. It is therefore interpreted as related to the formation of the mafic-ultramafic section itself preserved in this ophiolite.

The metagabbros of the lower slice contain a main population of igneous zircons that have provided a U-Pb protolith age of c. 602 Ma (Fig. 5). These zircons also show a resetting episode with minor crystallisation of new zircon at c. 540 Ma, which is interpreted as the age of deformation and metamorphism of the ophiolite and eventually the obduction of the ophiolite over the Serie Negra (Arenas et al. 2018). This age is somewhat younger than the age obtained for the deformation of the Serie Negra in the northern sector of the Ossa Morena Complex (c. 550-560 Ma; Blatrix and Burg 1981, Dallmeyer and Quesada 1992).

3.1.2. Element and isotope geochemistry

Whole-rock chemical analyses of the lower slice gabbros can be found in Arenas et al. (2018). The projection of their compositions on the Nb/Y-Zr/Ti diagram (Pearce 1996; Fig. 6) allows them to be classified as common sub-alkaline mafic types, with moderate compositional variability. In the AFM diagram (Irvine and Baragar, 1971; Fig. 6) they stand out for their high MgO contents, characteristic of tholeiitic boninitic magmas (Dobson et al. 2006). The REE contents are very low, with unfractionated chondrite-normalised patterns (Nakamura 1974) showing lower values than chondrite for the light REEs and somewhat higher for the heavy REEs, with marked positive Eu anomalies (Fig. 6). All samples are distinctly boninitic types in the TiO_2-MnO-P_2O_5 diagram (Mullen 1983; Fig. 6), and with supra-subduction zone (SSZ) signature in the Nb/Y-Th/Yb diagram (Shervais 1982, Pearce 2008, 2014; Fig. 7), akin to primitive oceanic arcs. The boninitic character of these gabbros is also evident in the Ti-V (Shervais 1982, Pearce 2014; Fig. 7) and Ti/V-Th/Nb (Shervais 2022; Fig. 8) diagrams. Finally, the average composition of the gabbros shows very depleted HFSE contents relative to N-MORBs (Pearce 2014; Fig. 9), which is again characteristic of boninitic magmas. Boninitic types are considered to be slab-proximal magmas characteristic of magmatic arc settings, especially of the fore-arc regions (Crawford et al., 1981, Hickey and Frey, 1982, Pearce 2014).

On the other hand, the superchondritic εHf(t) >11 of zircons from the gabbros (Arenas et al. 2018) fall in the MORB-depleted mantle field (Fig. 10. It can be thence surmised that zircon crystallized from mafic magmas that were almost directly derived from a depleted mantle source.

3.2. Mérida Ophiolite

3.2.1. Regional setting, lithologies and geochronology

The Mérida Ophiolite is part of the Mérida Massif, located north of the Ossa-Morena Complex (Fig. 3). This massif consists of three terranes with different origin and tectonothermal evolution (Fig. 4; Díez Fernández et al. 2022). Above the intermediate ophiolitic terrane, an upper terrane includes a thick siliciclastic series corresponding to the

Montemolín Formation of the Serie Negra. This series contains a basal section where a dense network of diabases and microgabbros was emplaced, and is also intruded by numerous large massifs of tonalites and granites of varied composition, with a minor presence of gabbroic types (Fig. 4). The tonalite-granite massifs range in age from c. 600 Ma to c. 540 Ma (Rojo-Pérez et al. 2022). This assemblage appears in general moderately deformed and with a low grade metamorphic inprint. However, its basal section does show intense deformation reaching mylonitic and ultramylonitic characteristics at the contact with the Mérida Ophiolite, which is interpreted as a large extensional detachment (Trujillanos Detachment; Fig. 4; Díez Fernández et al. 2022). Below the mafic-ultramafic unit, the contact with the so-called Magdalena Gneisses terrane of continental affinity is also characterrized by intense mylonitic deformation, which in this case has been interpreted as a thrust (Magdalena Thrust; Fig. 4; Díez Fernández et al., 2022). These gneisses have a monotonous felsic composition, intense deformation and high-T metamorphic conditions with evidence of having reached partial melting.

The Mérida ophiolite consists of three different slices that together have a thickness of c. 3000 m (Fig. 4; Díez Fernández et al. 2022; Arenas et al. In press). The intermediate slice is the thicker one, which mainly consists of gabbros, banded gabbros, pegmatoid gabbros, hornblendites and diabases. The uppermost slice also contains a thin basal layer of serpentinised ultrabasic rocks, while a few metric scale granitoid intrusions have been found in the lower slice. The ophiolite is in general moderately deformed, with regional foliation development under amphibolite facies conditions. Igneous minerals are generally not preserved, with widespread replacement of the original ferromagnesian minerals by metamorphic amphiboles. In some sectors, typically below the basal thrusts of each slice, layers of medium to coarse-grained amphibolites and garnet-bearing amphibolites occur. The garnets have a synkinematic or tardi-kinematic character and reach up to 1 cm in diameter. Locally, the garnet amphibolites show evidence of partial melting. Considering the local character of the garnet amphibolites, and their development linked to the contact between the ophiolite slices, they have been interpreted as metamorphic soles formed by heating of gabbroic sections stacked under sections of lithospheric mantle, which would have been only partly preserved. The peak metamorphic conditions of the soles reached c. 700 °C and 8 kbar (c. 25km), along a P-T path with the characteristics of subduction inception (Arenas et al. In press). The development of such local heating and burial necessarily implies a priori the accretion of very hot material of buoyant nature, and therefore a short time lag between the generation of the oceanic lithosphere and subduction initiation (e.g. Garber et al. 2020, and references therein).

U-Pb dating of zircons obtained from a mildy deformed coarse-grained metagabbro yielded a concordia age of c. 594 Ma, which is interpreted as the age of mafic protoliths (Fig. 5; Arenas et al. In press). On the other hand, zircons from small granite bodies intruding the lower slice of the ophiolite yielded a U-Pb age of c. 565 Ma, which is also considered a protolith age which is much younger than the age of the mafic rocks, excluding a cogenetic character of both types of lithologies (Arenas et al. In press). In addition, a U-Pb age of garnets from the metamorphic sole in the vicinity of the Albarregas River, in the Mérida City, yielded a discordia line in a Tera-Wasserburg diagram with an age of 590 Ma (MSWD = 1.09; Fig. 11; Arenas et al. In press). The age of this garnet is only slightly younger than the formation of the mafic protoliths in the Merida Ophiolite, probably also resulting in a direct dating of the accretion of the ophiolite slices in an subduction initiation setting that triggered high-T metamorphism and development of the metamorphic soles, likely shortly followed by the accretion of the lower unit Magdalena Gneisses terrane in the same environment (Arenas et al. In press).

3.2.2. Element and isotopic geochemistry

Whole-rock chemical analyses of representative metagabbros of the Merida ophiolite have been published by Arenas et al. (In press). In the Nb/Y-Zr/Ti diagram (Pearce 1996; Fig. 6), these rocks are subalkaline mafic types with some compositional variability, somewhat greater than that shown by the mafic rocks of the Calzadilla Ophiolite. In the AFM diagram (Irvine and Baragar, 1971; Fig. 6) they show a greater diversity, with significant variations in FeO and MgO contents but with a group of samples comparable to those of the

Calzadilla Ophiolite. The REE contents are moderate, although much higher than the chondritic ones, with normalized patterns (Nakamura 1974) showing no fractionation (Fig. 6). The REE contents and patterns of the gabbros from the Mérida Ophiolite are clearly different from their counterparts in the Calzadilla Ophiolite (Fig. 6). The relative compositional variability of these mafic rocks is illustrated in both the TiO_2-MnO-P_2O_5 diagram (Mullen 1983; Fig. 6) and the Nb/Y-Th/Yb diagram (Shervais 1982, Pearce 2008, 2014; Fig. 7), which however also show their SSZ signature with a higher continental influence than in the Calzadilla Ophiolite. The mafic rocks of both ophiolites are well differentiated in the Ti-V (Shervais 1982, Pearce 2014; Fig. 7) and Ti/V-Th/Nb (Shervais 2022; Fig. 8) diagrams. The average values of both mafic rock groups normalised to N-MORB (Pearce 2014; Fig. 9) are also rather different. The composition of the mafic rock of the Merida Ophiolite is characteristic of SSZ magmas generated in subduction settings, as indicated by the HFSE contents and negative anomalies in Ta+Nb, Hf+Zr and Ti (Pearce 2014; Fig. 9). The geochemical characteristics of the gabbroic rocks of the Calzadilla and Mérida ophiolites are clearly distinct, although both assemblages share a common peri-Gondwanan SSZ setting. Considering their compositional characteristics, the structure of the Mérida Massif, where the ophiolitic unit is located between two continental units, and the position closer to the Central Iberian Zone (North of the Ossa-Morena Complex; Fig. 3), we suggest that the Mérida Ophiolite formed in relation to the opening of a back-arc basin. This interpretation suggests two similar but distinguishable SSZ environments for the Ediacaran ophiolites of the SW Iberian Massif, which would have been generated roughly synchronously in a fore-arc (Calzadilla Ophiolite) and a back-arc (Mérida Ophiolite) (Arenas et al. 2018, In press; Díez Fernández et al. 2019, 2022).

The Hf isotopic systematics zircons separated from the mafic rocks of the Mérida Ophiolite is characteristic of juvenile magmas in equilibrium with a depleted mantle of their age (Arenas et al. In press; Fig. 10). The ƐHf(t) values for the considered U-Pb ages are lower than those of the mafic rocks of the Calzadilla Ophiolite. Still much lower are the ƐHf(t) of zircons of the granitic rocks found in the lower slice of the Merida Ophiolite (Arenas et al.

In press; Fig. 10), indicating contrasted isotopic sources and origins for both types of magmas. Together with their contrasted protolith ages, these data indicate that the granitic rocks formed in a magmatic arc and intruded the mafic rocks long after their formation in a peri-Gondwana back-arc and their metamorphism, deformation and emplacement upon the closure of the back-arc (Arenas et al. In press).

4. The origin of Cadomia

4.1. The regional approach

The Ossa-Morena Complex contains a section of the outer margin of Gondwana. The Ediacaran series of the so-called Serie Negra were deposited in this margin. This is the main metasedimentary sequence related to the ophiolites of the SW Iberian Massif. Within the Ossa-Morena Complex, the Calzadilla Ophiolite occupies a more southerly position (Fig. 3), closer former outer boundary of the Gondwanan palaeo-margin. In contrast, the Mérida Ophiolite has a more northerly position, closer to the autochthonous Central Iberian Zone (Fig. 3), interpreted in general terms as a broad Ediacaran back-arc basin (Fuenlabrada et al. 2020 and references therein). The structural relationships of the Calzadilla and Mérida ophiolites with the Ediacaran series are contrasted. While the former is interbedded with these series and was finally emplaced on top of them (Fig. 4), the latter occurs accreted beneath the Ediacaran series and thrusted on a gneissic section that has been interpreted as an inland section of the Gondwanan palaeo-margin (Fig. 4; Díez Fernández et al. 2022, Arenas et al. In press). The Calzadilla Ophiolite has a low to medium-T syn-accretionary tectonothermal evolution (Arenas et al. 2018), that indicates a relatively cold emplacement during thrusting which must therefore have occurred considerably after the formation of the ophiolite protoliths. In contrast, the Mérida Ophiolite shows local evidence of the development of high-T metamorphic soles, with garnet generation and partial melting (Arenas et al. In press). This can be better interpreted as relation to the obduction of buoyant material shortly after oceanic lithosphere formation in the back-arc. Therefore, it seems clear that the Calzadilla and Mérida ophiolites show contrasted characteristics in their regional position, relations to the Ediacaran series, lithological constitution and tectonothermal evolution (Fig. 4).

The U-Pb ages of zircons of the metagabbros of both ophiolites also confirms their different, but close, chronology. The metagabbros of the Calzadilla Ophiolite formed at c. 602 Ma (Fig. 5; Arenas et al. 2018), while in the Mérida Ophiolite are slightly younger, c. 594 Ma (Fig. 5; Arenas et al. In press). On the other hand, metamorphic sole formation at c. 590 Ma in the Mérida Ophiolite (Fig. 11; Arenas et al. In press), confirms a rapid evolution and of the corresponding oceanic lithosphere. That the mafic rocks of both ophiolites represent juvenile magmas in equilibrium with the depleted mantle of their age is demonstrated by the Hf isotopic composition of zircon (Fig. 10), as opposed to the older isotopic sources of the granitoids that intrude the Mérida Ophiolite and those emplaced in the peri-Gondwanan Ediacaran magmatic arc (Fig. 10; Rojo-Pérez et al. 2022, Arenas et al. In press).

The geochemical characteristics of the Calzadilla and Merida ophiolites are different. The mafic rocks of both ophiolites have compositions characteristic of magmas formed in supra-subduction zone settings. However, the mafic rocks of the Calzadilla Ophiolite correspond to extremely REE- and HFSE-depleted boninitic magmas (Figs. 6, 7, 8, 9). In contrast, the mafic rocks of the Mérida Ophiolite are more akin to arc-tholeiites with higher REE and HFSE contents (Figs. 6, 7, 8, 9). The extreme low content in incompatible trace elements of boninitic magmas is the result of previous melting events that removed most of the incompatible elements from the residual mantle source. It is considered that boninitic magmas developed from an ultra-depleted harzburgite source (Crawford et al. 1981; Hickey and Frey 1982). Most boninite magmas are formed in fore-arc settings or in the embryonic stages of magmatism associated with the splitting of an island arc and the generation of a back-arc basin (Cameron et al. 1979). The African margin of Gondwana has acted as an active margin in different stages dated between c. 750-500 Ma, forming the Avalonian-Cadomian volcanic arc (Fuenlabrada et al. 2020, Andonaegui et al. 2016, Arenas et al. 2016a). The fore-arc regions are characteristically subject to repeated cycles of opening of extensional basins in supra-subduction zone settings (Wilson, 1989). Considering this peri-

Gondwanan setting and also taking into account the position of the Calzadilla Ophiolite and its emplacement relations with the Ediacaran series, it seems likely that the generation of its boninitic magmas took place in a fore-arc setting. On the contrary, the geochemical characteristics of the mafic rocks of the Merida Ophiolite, and the type of structural relationships shown by this ophiolite with the Ediacara series and the underlying gneissic terrane, seem more compatible with its generation in a peri-Gondwanan back-arc setting.

A geodynamic model is presented in Figure 12 and may explain the generation of the Calzadilla and Merida ophiolites in the context of the evolution of the NW African Gondwanan margin. This view is based on regional, geochronological, geochemical and tectonothermal evolution of both ophiolites. The model considers the initial opening of a fore-arc basin in peri-Gondwana (c. 602 Ma; protoliths of the Calzadilla Ophiolite; Fig. 12a), followed by the opening of a back-arc basin (c. 594; protoliths of the Merida Ophiolite; Fig. 12b). The opening of the back-arc basin favors the drift of a section of unknown size of the outermost active margin of Gondwana, which is considered to be the Cadomian plate (Fig. 12b). Somewhat later (c. 590 Ma), in accordance with the tectonothermal evolution recorded in the Merida Ophiolite, the accretion of this ophiolite beneath the drifted continental section, the closure of the peri-Gondwana oceanic domain and the collision and final emplacement of this element with the continent would have occurred (Fig. 12c). The evolution of this peri-Gondwana section would continue with the progression of deformation towards the outermost margin and the final obduction of the Calzadilla Ophiolite (c. 540 Ma), in part contemporaneous with the initial collapse of the volcanic arc and before its subsequent reactivation during the deposition of the unconformable Malcocinado Formation (c. 534 Ma; Fig. 12d). The entire collisional section has been considered the final Cadomian domain, in accordance with its present-day location in the basement of Central and Western Europe, where it has traditionally been described as Cadomian basement (D’Lemos et al. 1990).

4.2. The geodynamic approach

The geodynamic evolution undergone by the Cadomian basement is still a matter of debate because geological constraints at the global scale remains relatively poor for this remote time. Plate tectonic reconstructions have been proposed (Stampfli et al. 2011, 2013, von Raumer et al. 2013, 2015, 2017), which include the Ossa-Morena area in a global framework, but from the Early Phanerozoic “only”. Recently however, a new global plate tectonic model (Vérard, 2019a, 2019b) — the PANALESIS model — has been released (Vérard, 2021) that proposes a scenario for the geodynamic evolution of the Earth back to the Tonian time (Early NeoProterozoic). In this model, a proto-Cadomia continental ribbon detached from a continental area which included North China. The new Cadomia plate evolved and is responsible for the collision of the Souttoufides in the High-Atlas at around 660–650 Ma (Villeneuve et al. 2015) and along the Bassarides at 650–640 Ma (Villeneuve, 1984, 2005, Gasquet et al. 2005, 2008, Villeneuve et al. 2006, 2010). The Cadomia plate however keeps on sliding along Western Africa and eventually detaches again from proto-Gondwana at around 630 Ma.

At ca. 620 Ma, the Nethuns Arc, related to an intra-oceanic subduction zone, detached from a continental zone containing South China (Fig. 13a). Although the time resolution of the model is considered to be that of the interval between subsequent time slices (i.e. every 10 Myrs), the model suggests an age for the Nethuns Arc collision compatible with the 596 Ma U-Pb age proposed herein for the formation of the Mérida Ophiolite. The Cadomia – Nethuns collision triggered the inversion of the passive margin of Cadomia into an active margin. Tectonically speaking, one hypothesis may thus be that the Calzadilla Ophiolite formed part of the plate located north of Cadomia, whereas the Mérida Ophiolite was associated with the oceanic domain located to the north of West Africa Craton. Figure 13a shows the approximated location suggested for the SW Iberia Cadomian ophiolites, although the time resolution of the model is 10 Myrs. Alternate solutions however must be further investigated.

Be that as it may, the Qilian continental ribbon, detached from North China at ca. 580 Ma (Fig. 13b), obliquely (tranpressionally) collided with Cadomia around 560 Ma (Fig. 13c). The collision triggered the closing of the oceanic basin between Cadomia/Qilian and the (West) proto-Gondwana margin, closing which ended up at around 540 Ma (Fig. 13d) with the High-Atlas/Qinling collision. The subsequent evolution (from the Cambrian onwards) can be found, for instance, in Stampfli et al. (2013).

5. Discussion

The recent discovery of the Calzadilla and Mérida oceanic terranes in the SW Cadomian basement of the Iberian Massif provides a new scenario for the evolution of this region. The origin of the Cadomian basement of Central and Western Europe has been considered related to the activity of a peri-Gondwanan volcanic arc, located at the periphery of the West African Craton and the Saharan Craton (Linnemann et al. 2014, Rojo-Pérez et al. 2021, Fuenlabrada et al. 2020). The new data however confirm the involvement of one or more oceanic domains, as would have been expected whose existence can be placed at least, based on existing geochronological data, in the interval 600-540 Ma (Arenas et al. 2018, In press). The two ophiolites identified are of supra-subduction zone type, although the mafic rocks of the Calzadilla Ophiolite have geochemical characteristics similar to those formed in fore-arc basins, while the mafic rocks of the Mérida Ophiolite are similar to those formed during the opening of back-arc basins. The absence of mafic rocks with MORB composition suggests that the participating oceanic areas were rather small in extent, but it is known that the oceanic lithosphere of large oceanic basins rarely survives subduction, calling for caution in this point (Pearce et al. 1984, Dilek and Furnes 2014, Arenas et al. 2021). The final extent reached by the oceanic domain represented by the Merida Ophiolite cannot be known on the basis of existing regional data. Refined provenance work can provide clues on the original location of the rifted peri-Gondwanan section (Díez Fernández et al., 2010, Linnemann et al 2014, Albert et al. 2015, Rojo-Pérez et al. 2021), but not on the extent of its drift.

Isotopic chronology data on the tectonothermal evolution of the Calzadilla and Mérida ophiolites and nearby series are very scarce. Even so, these are the data needed to handled the chronology of the closure of the oceanic domains involved. To date, they indicate that the Mérida Ophiolite was accreted at high temperatures shortly after its formation (c. 590

Ma; U-Pb dating of garnet), whereas the Calzadilla Ophiolite was obducted under greenschist facies conditions, probably long after the formation of its mafic protoliths (c. 540 Ma; U-Pb dating of zircon), and that the Ediacaran series of the Ossa-Morena Complex were deformed and metamorphosed in this time interval (560-550 Ma; 40Ar-39Ar; Blatrix and Burg 1981, Dallmeyer and Quesada 1992).

Consequently, regional geology can document that the evolution of the Cadomian basement of SW Iberia includes: 1) the activity of a volcanic arc that started before c. 600 Ma and developed over the siliciclastic Peri-Gondwanan platform (Serie Negra); 2) the opening of fore-arc and back-arc basins in the interval between 602 and 594 Ma, the extent of which cannot be estimated from regional data, and the subsequent rifting and drifting of a section of the continental margin including the volcanic arc (Cadomia); 3) the subsequent closure of the oceanic domains involved, the final collision of Cadomia with Gondwana and the obduction of the Calzadilla and Merida ophiolites in the interval between 590 and 540 Ma. The regional domain generated thus includes several continental and oceanic terranes with different tectonothermal origin and evolution. This domain currently represents the Cadomian basement of the Variscan Central and Western Europe.

The use of a global plate tectonic model for the time range considered allows analyzing from a theoretical point of view some of the issues that do not admit an interpretation based only on regional data. The PANALESIS model offered in this work shows a geodynamic scenario compatible with the Ediacaran rifting and drifting of a peri-Gondwanan terrane interpreted as Cadomia, as well as with the opening of a new oceanic domain of considerable amplitude towards the north of the West Africa Craton. Both facts are compatible with inferences made from regional geology and especially from the existence of Ediacaran ophiolites. The later closure of the oceanic domain and the final collision of Cadomia with Gondwana is also consistent with the interpretation based on regional data. The main Cadomian section would finally be located, according to the PANALESIS model, north of the West Africa Craton, where it is indeed located today. However, the major difference between the two datasets arises when comparing the time ranges, which show partial disagreement especially in the chronology of the Cadomia-Gondwana collision. Nevertheless, the comparison of the theoretical and regional models, together with their constant updating and the acquisition of new geochronological data, seems to be the appropriate procedure to improve the knowledge of the geodynamics of the peri-Gondwana realm in the considered time range.

The results obtained in this work clearly indicate that the Cadomian basement of Central and Western Europe is complex in nature. In its development, rifting and drifting of a large peri-Gondwanan terrain (Cadomia) and the opening of oceanic domains that may have reached a considerable extent must be considered. These oceanic domains were subsequently subducted, facilitating the final collision of Cadomia with Gondwana and the obduction of some of the oceanic lithospheric sections involved. The results obtained in the SW Iberian Massif can be extrapolated to other Cadomian basement regions of Europe, but the key element for future investigation is the possible exstence of ophiolitic units that have been overlooked in regional research.

Acknowledgments

Financial support has been provided by the Spanish projects PID2020-112489-GB-C21 and PID2020-112489-GB-C22, funded by MCIN/AEI. R.A. and A.G. acknowledge the financial support to FIERCE by the Wilhelm and Else Heraeus Foundation and the Deutsche Forschungsgemeinschaft. This paper is FIERCE contribution No. xxx.

Disclosure statement

No potential conflict of interest was reported by the authors.

Funding

Insightful revisions of the manuscript by Josep Maria Casas and Alexandre Kounov are kindly acknowledged. This work was supported by the Ministerio de Ciencia e Innovación (Spain), projects: PID2020-112489-GB-C21 and PID2020-112489-GB-C22. R.A. and A.G. acknowledge the financial support to FIERCE by the Wilhelm and Else Heraeus Foundation and the Deutsche Forschungsgemeinschaft. This paper is FIERCE contribution No. XXX.

References

Albert, R., Arenas, R. Gerdes, A., Sánchez Martínez, S. and Marko, L. 2015. Provenance of the HP-HT subducted margin in the Variscan belt (Cabo Ortegal Complex, NW Iberian Massif). *Journal of Metamorphic Geology*, **33**, 959-979.

Andonaegui, P., Arenas, R., Albert, R., Sánchez Martínez, S., Díez Fernández, R. and Gerdes, A. 2016. The last stages of the Avalonian-Cadomian arc in NW Iberian Massif: isotopic and igneous record for a long-lived peri-Gondwanan magmatic arc. *Tectonophysics*, **681**, 6-14.

Arenas, R., Martínez Catalán, J.R., Sánchez Martínez, S., Fernández-Suárez, J., Andonaegui, P., Pearce, J.A. and Corfu, F. 2007. The Vila de Cruces Ophiolite: A remnant of the early Rheic Ocean in the Variscan suture of Galicia (NW Iberian Massif). *Journal of Geology*, **115**, 129-148.

Arenas, R., Sánchez Martínez, S., Gerdes, A., Albert, R., Díez Fernández, R. and Andonaegui, P. 2014*a*. Re-interpreting the Devonian ophiolites involved in the Variscan suture: U-Pb and Lu-Hf zircon data of the Moeche Ophiolite (Cabo Ortegal Complex, NW Iberia). *International Journal of Earth Sciences*, **103**, 1385-1402.

Arenas, R., Díez Fernández, R., Sánchez Martínez, S., Gerdes, A., Fernández-Suárez, J. and Albert, R. 2014*b*. Two-stage collision: Exploring the birth of Pangea in the Variscan terranes. *Gondwana Research*, **25**, 756-763.

Arenas, R., Sánchez Martínez, S., Díez Fernández, R., Gerdes, A., Abati, J., Fernández-Suárez, J., Andonaegui, P., González Cuadra, P., López Carmona, A., Albert, R., Fuenlabrada, J.M. and Rubio Pascual, F.J. 2016*a*. Allochthonous terranes involved in the Variscan suture of NW Iberia: A review of their origin and tectonothermal evolution. *Earth-Science Reviews*, **161**, 140-178.

Arenas, R., Díez Fernández, R., Rubio Pascual, F.J., Sánchez Martínez, S., Martín Parra, L.M., Matas, J., González del Tánago, J., Jiménez-Díaz, A., Fuenlabrada, J.M., Andonaegui, P. and García-Casco, A., 2016*b*, The Galicia – Ossa-Morena Zone:

Proposal for a new zone of the Iberian Massif. Variscan Implications. *Tectonophysics*, **81**, 135-143.

Arenas, R., Fernández-Suárez, J., Montero, P., Díez Fernández, R., Andonaegui, P., Sánchez Martínez, S., Albert, R., Fuenlabrada, J.M., Matas, J., Martín Parra, L.M., Rubio Pascual, F.J., Jiménez-Díaz, A. and Pereira, M.F. 2018. The Calzadilla Ophiolite (SW Iberia) and the Ediacaran fore-arc evolution of the African margin of Gondwana. *Gondwana Research*, **58**, 71-86.

Arenas, R., Sánchez Martínez, S., Albert, R., Haissen, F., Fernández-Suárez, F.,Pujol-Solá, N., Andonaegui, P., Díez Fernández, R., Proenza, J.A., Garcia-Casco, A. and Gerdes, A. 2021. 100 myr cycles of oceanic lithosphere generation in peri-Gondwana: Neoproterozoic–Devonian ophiolites from the NW African-Iberian margin of Gondwana and the Variscan Orogen. *Geological Society, London, Special Publications*, **503**, 169-184.

Arenas, R., Rojo-Pérez, E., Díez Fernández, R., Albert, R., Novo-Fernández, I., Sánchez Martínez, S., Fuenlabrada, J.M., Andonaegui, P., Moreno-Martín, D., Gerdes, A. and Garcia-Casco, A. In press. Opening and closure of Cadomian peri-Gondwanan oceans: age and evolution of the Mérida Ophiolite (SW Iberia). *International Geology Review*. https://doi.org/10.1080/00206814.2022.2129475

Azor, A., Rubatto, D., Simancas, J.F., González Lodeiro, F., Martínez Poyatos, D., Martín Parra, L.M. and Matas, J. 2008. Rheic Ocean ophiolitic remnants in southern Iberia questioned by SHRIMP U-Pb zircon ages on the Beja-Acebuches amphibolites. *Tectonics*, **27**, TC5006.

Bandrés, A. 2001. Evolución geodinámica poliorogénica de los dominios septentrionales de la ZOM. *PhD. Thesis. Universidad del País Vasco, Bilbao, Spain*, 377 p.

Bandrés, A., Eguíluz, L., Pin, C., Paquette, J.L., Ordóñez, B., Le Fèvre, B., Ortega, L.A. and Gil Ibarguchi, J.I. 2004. The northern Ossa-Morena Cadomian batholith (Iberian Massif): Magmatic arc origin and early evolution. *International Journal of Earth Sciences,* **93**, 860-885.

Blatrix, P. and Burg, J.P. 1981. 40Ar/39Ar dates from Sierra Morena (Southern Spain): Variscan metamorphism and Cadomian orogeny. *Neus Jahrb. Mineral. Monatshefte*, **10**, 470-478.

Blichert-Toft, J. and Albarède, F. 2008. Hafnium isotopes in Jack Hills zircons and the formation of the Hadean crust. *Earth and Planetary Science Letters*, **265**, 686–702.

Cameron, W.E., Nisbet, E.G. and Dietrich, V.J. 1979. Boninites, komatiites and ophiolitic basalts. *Nature*, **280**, 550-553.

Carvalhosa, A. 1965. Contribuição para o conhecimento geológico da região entre Portel e Ficalho (Alentejo). *Memorias dos Serviços Geológicos de Portugal, Nova Série*, **11**, 1-32.

Clark, A.H., Scott, D.J., Sandeman, H.A., Bromley, A.V. and Farrar, E. 1998. Siegenian generation of the Lizard ophiolite: U-Pb zircon age data for plagiogranite, Porthkerries, Cornwall. *Journal of de Geological Society, London*, **155**, 595-598.

Crawford, A.J., Beccaluva, L. and Serri, G. 1981. Tectonomagmatic evolution of the West Philippine-Mariana region and the origin of boninites. *Earth Planetary Science Letters*, **54**, 346-356.

D'Lemos, R.S., Strachan, R.A. and Topley, C.G. 1990, The Cadomian orogeny in the North Armorican Massif: a brief review. *Geological Society, London, Special Publications*, **51**, 3-12.

Dallmeyer, R.D. and Quesada, C. 1992. Cadomian vs. Variscan evolution of the Ossa-Morena zone (SW Iberia): field and 40Ar/39Ar mineral age constraints. *Tectonophysics*, **216**, 339-364.

Díaz García, F., Arenas, R., Martínez Catalán, J.R., González del Tánago, J. and Dunning, G.R. 1999. Tectonic evolution of the Careón Ophiolite (northwest Spain): a remnant of oceanic lithosphere in the Variscan Belt. *Journal of Geology*, **107**, 587-605.

Díez Fernández, R., Martínez Catalán, J.R., Gerdes, A., Abati, J., Arenas, R. and Fernández-Suárez, J. 2010. U-Pb ages of detrital zircons from the basal allochthonous units of NW Iberia: Provenance and paleoposition on the northern margin of Gondwana during the Neoproterozoic and Paleozoic. *Gondwana Research*, **18**, 385-399.

Díez Fernández, R. and Arenas, R. 2015. The Late Devonian Variscan suture of the Iberian Massif: A correlation of high-pressure belts in NW and SW Iberia. *Tectonophysics*, **654**, 96-100.

Díez Fernández, R., Arenas, R., Pereira, M.F., Sánchez-Martínez, S., Albert, R., Martín Parra, L.M., Rubio Pascual, F.J. and Matas, J. 2016. Tectonic evolution of Variscan Iberia: Gondwana-Laurussia collision revisited. *Earth-Science Reviews*, **162**, 269-292.

Díez Fernández, R., Jiménez-Díaz, A., Arenas, R., Pereira, M.F. and Fernández-Suárez, J. 2019. Ediacaran obduction of a fore-arc ophiolite in SW Iberia: A turning point in the evolving geodynamic setting of peri.Gondwana. *Tectonics*, **38**, 95-119.

Díez Fernández, R., Arenas, R., Rojo-Pérez, E., Sánchez Martínez, S. and Fuenlabrada, J.M. 2022. Tectonostratigraphy of the Mérida Massif reveals a new Cadomian suture zone exposure in Gondwana (SW Iberia). *International Geology Review*, **64**, 405-424.

Dilek, Y. and Furnes, H. 2014. Ophiolites and their origin. *Elements*, **10**, 93-100.

Dobson, P.F., Blank, J.G., Maruyama, S. and Liou, J.G. 2006. Petrology and geochemistry of boninite-series volcanic rocks, Chichi-Jima, Bonin Islands, Japan. *International Geology Review*, **48**, 669-701.

Eguiluz, L. 1988. Petrogénesis de rocas ígneas y metamórficas en el antiforme de Burguillos-Monesterio. Macizo Ibérico Meridional. *PhD. Thesis. Universidad del País Vasco, Bilbao, Spain*, 649 p.

Eguiluz, L., Gil Ibarguchi, J.I., Ábalos, B. and Apraiz, A. 2000. Superposed Hercynian and Cadomian orogenic cycles in the Ossa-Morena zone and related areas of the Iberian Massif. *Geological Society of America Bulletin*, **112**, 1398-1413.

El Hadi, H., Simancas, J.F., Martínez Poyatos, D., Azor, A., Tahiri, A., Montero, P., Fanning, C.M., Bea, F. and González-Lodeiro, F. 2010. Structural and geochronological constraints on the evolution of the Bou Azzer Neoproterozoic ophiolite (Anti-Atlas, Morocco). *Precambrian Research*, **182**, 1-14.

Fricke, W. 1941. Die Geologie des Grenxebietes zwischen nordöstlicher Sierra Morena und Extremadura. *PhD. Thesis. University of Berlin, Berlin, Germany*, 91 p.

Fuenlabrada, J.M., Arenas, R., Sánchez Martínez, S., Díez Fernández, R., Pieren, A.P., Pereira, M.F., Chichorro, M. and Silva, J.B. 2020. Geochemical and isotopic (Sm-Nd) provenance of Ediacaran-Cambrian metasedimentary series from the Iberian Massif. Paleoreconstruction of the North Gondwana margin. *Earth-Science Reviews*, **201**, 103079.

Garber, J.M., Rioux, M., Kylander-Clark, A.R.C., Hacker, B.R., Vervoort, J.D. and Searle, M.P. 2020. Petrochronology of Wadi Tayin metamorphic sole metasediment, with implications for the thermal and tectonic evolution of the Samail Ophiolite (Oman/UAE). *Tectonics*, **39 (12)**, e2020TC006135

Gasquet, D., Levresse, G., Cheilletz, A., Azizi-Samir, M. R. and Mouttaqi, A. 2005. Contribution to a geodynamic reconstruction of the Anti-Atlas (Morocco) during Pan-African times with the emphasis on inversion tectonics and metallogenic activity at the Precambrian-Cambrian transition. *Precambrian Research*, **140**, 157–182.

Gasquet, D., Ennih, N., Liégeois, J.-P., Soulaimani, A. and Michard, A. 2008. The Pan-African belt. The Geology Of Morocco. *Lectures Notes in Earth Sciences, Springer-Verlag Berlin Heidelberg publisher,* **116**, 33–64.

Gonzalo, J.C. 1987. Petrología y estructura del Basamento en el área de Mérida (Extremadura Central). *PhD. Thesis. Universidad de Salamanca, Spain*, 327 p.

Hodel, F., Triantafyllou, A., Berger, J., Macouin, M., Baele, J.-M., Mattielli, N., Monnier, C., Trindade, R.I.F., Ducea, M.N., Chatir, A., Ennih, N., Langlade, J. and Poujol, M. 2020. The Moroccan Anti-Atlas ophiolites: Timing and melting processes in an intra-oceanic arc-back-arc environment. *Gondwana Research*, **86**, 182-202.

Hickey, R.L. and Frey, F.A. 1982. Geochemical characteristics of boninite series volcanics: implications for their source. *Geochimica et Cosmochimica Acta*, **46**, 2099-2115.

Irvine, T.N. and Baragar, W.R.A. 1971. A guide to the chemical classification of the common volcanic rocks. *Canadian Journal of Earth Sciences*, **8**, 523-548.

Kroner, U. and Romer, R.L. 2013. Two plates - Many subduction zones: The Variscan orogeny reconsidered. *Gondwana Research*, **24**, 298-329.

Liégeois, J.P., Black, R., Navez, J. and Latouche, L. 1994. Early and Late Pan-African orogenies in the Aïr assembly of terranes (Tuareg shield, Niger). *Precambrian Research*, **67**, 59-88.

Linnemann, U., Pereira, M.F., Jeffries, T., Drost, K. and Gerdes, A. 2008. Cadomian Orogeny and the opening of the Rheic Ocean: New insights in the diachrony of geotectonic processes constrained by LA-ICP-MS U-Pb zircon dating (Ossa-Morena and Saxo-Thuringian Zones, Iberian and Bohemian Massifs). *Tectonophysics*, **461**, 21-43.

Linnemann, U., Gerdes, A., Hofmann, M. and Marko, L. 2014. The Cadomian Orogen: Neoproterozoic to Early Cambrian crustal growth and orogenic zoning along the periphery of the West African Craton – constraints from U-Pb zircon ages and Hf isotopes (Schwarzburg Antiform, Germany). *Precambrian Research*, **244**, 236-278.

Liñán, E. 1984. Los icnofósiles de la Formación Torreárboles (Precámbrico? – Cámbrico) en los alrededores de Fuente Cantos, Badajoz. *Cuadernos del Laboratorio Xeolóxico de Laxe*, **8**, 283-314.

Martínez Catalán, J.R., Arenas, R., Abati, J., Sánchez Martínez, S., Díaz García, F., Fernández-Suárez, J., González Cuadra, P., Castiñeiras, P., Gómez Barreiro, J., Díez Montes, A., González Clavijo, E., Rubio Pascual, F.J., Andonaegui, P., Jeffries, T.E., Alcock, J.E., Díez Fernández, R. and López Carmona, A. 2009. A rootless suture and the loss of the roots of a mountain chain: The Variscan belt of NW Iberia. *Comptes Rendus Geoscience*, **341**, 114-126.

Martínez Catalán, J.R., Collett, S., Schulmann, K., Aleksandrowski, P. and Mazur, S. 2020. Correlation of allochthonous terranes and major tectonostratigraphic domains between NW Iberia and the Bohemian Massif, European Variscan belt. *International Journal of Earth Sciences*, **109**, 1105-1131.

Merinero, R., Lunar, R., Ortega, L., Piña, R., Monterrubio, S. and Gervilla, F. 2013. Hydrothermal palladium enrichment in podiform chromitites of Calzadilla de los Barros (SW Iberian Peninsula). *Canadian Mineralogist*, **51**, 387-404.

Merinero, R., Lunar, R., Ortega, L., Piña, R., Monterrubio, S. and Gervilla, F. 2014. Zoned chromite records multiple metamorphic episodes in the Calzadilla de los Barros ultramafic bodies (SW Iberian peninsula). *European Journal of Mineralogy*, **26**, 757-770.

Mullen, E.D. 1983. MnO/TiO2/P2O5: a minor element discriminant for basaltic rocks of oceanic environments and its implications for petrogenesis. *Earth and Planetary Science Letters*, **62**, 53–62.

Murphy, J.B., Cousens, B.L., Braid, J.A., Strachan, R.A., Dostal, J., Keppie, J.D. and Nance, R.D. 2011. Highly depleted oceanic lithosphere in the Rheic Ocean: Implications for Paleozoic plate reconstructions. *Lithos*, **123**,165-175.

Nakamura, N. 1974. Determination of REE, Ba, Fe, Mg, Na and K in carbonaceous and ordinary chondrites. *Geochimica et Cosmochimica Acta*, **38**, 757-775.

Nance, R.D., Gutiérrez-Alonso, G., Keppi, J.D., Linnemann, U., Murphy, J.B., Quesada, C., Strachan, R.A. and Woodcock, N.H. 2010. Evolution of the Rheic Ocean. *Gondwana Research*, **17**,194-222.

Novo-Fernández, I., Arenas, R., Díez Fernández, R. and Garcia-Casco, A. In press. A complex accretionary assembly of Pangea developed in the range c. 400–340 Ma: the four successive events of high-P/ultra-high-P metamorphism of the Variscan Orogen. *International Geology Review*. https://doi.org/10.1080/00206814.2022.2127126.

Nutman, A.P., Green, D.H., Cook, C.A., Styles, M.T. and Holdsworth, R.E. 2001. SHRIMP U-Pb zircon dating of the exhumation of the Lizard Peridotite and its emplacement over crustal rocks: Constraints for tectonic models. *Journal of the Geological Society, London*, **158**, 809-820.

Pearce, J.A. 1996. A user's guide to basalt discrimination diagrams. *Geological Association of Canada Special Publication*, **12**, 79-113.

Pearce, J.A. 2008. Geochemical fingerprinting of oceanic basalts with applications to ophiolite classification and the search for archean oceanic crust. *Lithos*, **100**, 14-48.

Pearce, J.A. 2014. Immobile element fingerprinting of ophiolites. *Elements*, **10**, 101–108.

Pearce, J.A., Lippard, S.J. and Roberts, S. 1984. Characteristics and tectonic significance of supra-subduction zone ophiolites. *Geological Society, London, Special Publications*, **16**, 77–94.

Pereira, M.F. 2015. Potential sources of Ediacaran strata of Iberia: a review. *Geodinamica Acta*, **27**, 1-14.

Pereira, M.F., Chichorro, M., Linnemann, U., Eguiluz, L. and Silva, J.B. 2006. Inherited arc signature in Ediacaran and Early Cambrian basins of the Ossa-Morena Zone (Iberian Massif, Portugal): Paleogeographic link with European and North African correlatives. *Precambrian Research*, **144**, 297-315.

Pin, C., Paquette, J.L., Santos Zalduegui, J.F. and Gil Ibarguchi, J.I. 2002. Early Devonian supra-subduction zone ophiolite related to incipient collisional processes in the western Variscan Belt: The Sierra de Careón unit, Órdenes Complex, Galicia. *Geological Society of America Special Paper*, **364**, 57-71.

Pujol-Solá, N., Domínguez-Carretero, D., Proenza, J.A., Faouziya, H., Moha, I., González-Jiménez, J.M., Vanessa, C., Lhou, M. and Garcia-Casco, A. 2021. The chromitites of the Neoproterozoic Bou Azzer ophiolite (central Anti-Atlas, Morocco) revisited. Ore Geology Reviews, 134, 104166.

Quesada, C. 1990. Precambrian successions in SW Iberia: their relationship to Cadomian orogenic events. *Geological Society, London, Special Publications*, **51**, 553-562.

Rojo-Pérez, E., Fuenlabrada, J.M., Linnemann, U., Arenas, R., Sánchez Martínez, S., Díez Fernández, R., Martín Parra, L.M., Matas, J., Andonaegui, P. and Fernández-Suárez, J. 2021. Geochemistry and Sm–Nd isotopic sources of Late Ediacaran siliciclastic series in the Ossa-Morena Complex: Iberian-Bohemian correlations. *International Journal of Earth Sciences*, **110**, 467–485.

Rojo-Pérez, E., Linnemann, U., Hofmann, M., Fuenlabrada, J.M., Zieger, J., Fernández-Suárez, J., Andonaegui, P., Sánchez Martínez, S., Díez Fernández, R. and Arenas, R. 2022. U-Pb geochronology and isotopic geochemistry of adakites and related magmas in the well-preserved Ediacaran arc section of the SW Iberian Massif: the role of subduction erosion cycles in peri-Gondwanan arcs. *Gondwana Research*, **109**, 89-112.

Rojo-Pérez, E., Arenas, R., Fuenlabrada, J., Novo-Fernández, I., Sánchez Martínez, S., Moreno-Martín, D. and Díez Fernández, R. In press. Early Cambrian magmatism at SW Iberian section of the African-Gondwana margin: Geochemical and isotopic keys of an incipient tectonic switching. *Geological Society, London, Special Publications.*

Sánchez-García, T., Pereira, M.F., Bellido, F., Chichorro, M., Silva, J.B., Valverde-Vaquero, P., Pin, C. and Solá, A.R. 2013. Early Cambrian granitoids of North Gondwana margin in the transition from a convergent setting to intra-continental rifting (Ossa-Morena Zone, SW Iberia). *International Journal of Earth Sciences*, **103**, 1203-1218.

Sánchez Martínez, S., Arenas, R., Gerdes, A., Castiñeiras, P., Potrel, A. and Fernández-Suárez, J. 2011. Isotope geochemistry and revised geochronology of the Purrido Ophiolite (Cabo Ortegal Complex, NW Iberian Massif): Devonian magmatism with mixed sources and involved Mesoproterozoic basement. *Journal of the Geological Society, London*, **168**, 733-750.

Sánchez Martínez, S., Arenas, R., Albert, R., Gerdes, A. and Fernández-Suárez, J. 2021. Updated geochronology and isotope geochemistry of the Vila de Cruces Ophiolite: a case study of a peri-Gondwanan back-arc ophiolite. *Geological Society, London, Special Publications*, **503**, 497-530.

Sarrionandia, F., Ábalos, B., Errandonea-Martin, J., Eguíluz, L., Santos-Zalduegui, J.F., García de Madinabeitia, S., Carracedo-Sánchez, M. and Gil Ibarguchi, J.I. 2020. Ediacaran - Earliest Cambrian arc-tholeiite and adakite associations of the Malcocinado Formation (Ossa-Morena Zone, SW Spain): Juvenile continental crust and deep crustal reworking in northern Gondwana. *Lithos*, **372-373**, 105683.

Schäfer, H.J., Gebauer, D., Nägler, T.F. and Eguiluz, L. 1993. Conventional and ion-microprobe U-Pb dating of detrital zircons of the Tentudia Group (Serie Negra, SW Spain): implications for zircon systematics, stratigraphy, tectonics and the Precambrian/Cambrian boundary. *Contributions to Mineralogy and Petrology*, **113**, 289-299.

Schulmann, K., Edel, J.B., Martínez Catalán, J.R., Mazur, S., Guy, A. and Lardeaux, J.M., Ayarza, P. and Palomeras, I. 2022. Tectonic evolution and global crustal architecture of the European Variscan belt constrained by geophysical data. *Earth-Science Reviews*, **234**, article number 104195.

Shervais, J.W. 1982. Ti–V plots and the petrogenesis of modern and ophiolitic lavas. *Earth and Planetary Science Letters*, **59**, 101-118.

Shervais, J.W. 2022. The petrogenesis of modern and ophiolitic lavas reconsidered: Ti-V and Nb-Th. *Geoscience Frontiers*, **13**, 101319.

Stampfli, G.M., von Raumer, J. and Wilhem, C. 2011. The distribution of Gondwana-derived terranes in the Early Paleozoic. *Cuadernos del Museo Geominero,* **14**, 567-574.

Stampfli, G.M., Hochard, C., Vérard, C., Wilhem, C. and von Raumer, J. 2013. The formation of Pangea. *Tectonophysics,* **593**, 1-19.

Sun, S.S. and McDonough, W.F. 1989. Chemical and isotopic systematics of of oceanic basalts; implications for mantle composition and processes. in Saunders, A.D., and Norry, M.J., eds., Magmatism in the ocean basins. *Geological Society, London, Special Publications*, **42**, 313-345.

Taylor, S.R. and McLennan, S.M. 1985. The Continental Crust: its Composition and Evolution. Blackwell, Oxford.

Triantafyllou, A., Berger, J., Baele, J.-M., Bruguier, O., Diot, H., Ennih, N., Monnier, C., Plissart, G., Vandycke, S. and Watlet, A. 2018. Intra-oceanic arc growth driven by magmatic and tectonic processes recorded in the Neoproterozoic Bougmane arc complex (Anti-Atlas, Morocco). *Precambrian Research*, **304**, 39-63.

Vérard, C. 2019*a*. Plate tectonic modelling: Review and perspectives. *Geological Magazine*, **156**, 208-241.

Vérard, C. 2019*b*. Panalesis: Towards global synthetic palæogeographies using integration and coupling of manifold models. *Geological Magazine*, 156, 320-330.

Vérard, C. 2021. 888-444 Ma Global Plate Tectonic reconstruction with emphasis on the formation of Gondwana. *Frontiers in Earth Science*, **9**, 666153.

Villeneuve, M. 1984. Etude géologique de la bordure sud-ouest du craton ouest-africain. La suture pan-africaine et l'évolution des bassins sédimentaires protérozoïques et paléozoïques de la marge NW du continent de Gondwana. *PhD. Thesis. Universidad of Aix-Marseille, Aix-Marseille, France, 551 p.*

Villeneuve, M. 2005. Paleozoic basins in West Africa and the Mauritanide Thrust belt. *Journal of African Earth Sciences*, **43**, 166–195.

Villeneuve, M., Bellon, H., El Archi, A., Sahabi, M., Rehault, J.P., Olivet, J.L. and Aghzer, A. M. 2006. Evénements panafricains dans l'Adrar Souttouf (Sahara Marocain). *Comptes Rendus de l'Académie des Sciences, Geoscience*, **338**, 359–367.

Villeneuve, M., El Archi, A. and Nzamba, J. 2010. Les chaînes de la marge occidentale du Craton Ouest-Africain, modèles géodynamiques. *Comptes Rendus de l'Académie des Sciences, Geoscience*, **342**, 1–10.

Villeneuve, M., Gärtner, A., Youbi, N., El Archi, A., Vernhet, E., Rjimati, E.C., Linnemann, U., Bellon, H., Gerdes, A., Guillou, O., Corsini, M. and M Paquette, J.L. 2015. The southern and central parts of the "Souttoufide" belt, Northwest Africa. *Journal of African Earth Sciences*, **112**, 451–470.

von Raumer, J.F., Busy, F., Schaltegger, U., Schulz, B. and Stampfli, G.M. 2013. Pre-Mesozoic Alpine basements — Their place in the European Paleozoic framework. *Bulletin of the Geological Society of America*, **125**, 89-108.

von Raumer, J.F., Stampfli, G.M., Arenas, R. and Sánchez Martínez, S. 2015. Ediacaran to Cambrian oceanic rocks of the Gondwana margin and their tectonic interpretation. *International Journal of Earth Sciences*, **104**, 1107-1121.

von Raumer, J.F., Nesbor, H.D., Stampfli, G.M. 2017. The north-subducting Rheic Ocean during the Devonian: Consequences for the Rhohercynian ore sites. *International Journal of Earth Sciences*, **106**, 2279-2296.

Wedepohl, K.H. 1995. The compositions of the continental crust. *Geochimica and Cosmochimica Acta*, **59**, 1217–1232.

Wilson, M. 1989. Igneous Petrogenesis. A global tectonic approach. *Unwin Hyman Ltd, London*, 466 p.

Wojtulek, P.M., Schulz, B., Klemd, R., Gil, G., Dajek, M. and Delura, K. 2022. The Central-Sudetic ophiolites – Remnants of the SSZ-type Devonian oceanic lithosphere in the European part of the Variscan Orogen. *Gondwana Research,* **105**, 343-365.

Figure Captions

Figure 1. Reconstruction of a part of Pangaea at the end of the Paleozoic with distribution of orogens in the Baltica–Laurentia–Avalonia-–Gondwana junction. The general structure and domains of the Variscan Orogen is shown. Modified of Arenas et al. (2021). Pangaea map based on Martínez Catalán et al. (2009) and Díez Fernández and Arenas (2015). HP, high pressure.

Figure 2. Highly schematic reconstruction of the Anti Atlas–Iberia domain showing the probable distribution of the peri-Gondwanan ophiolites at the beginning of the Variscan deformation. Continuity of the ophiolites in the intermediate section between Avalonia and the Anti-Atlas is speculative, as most of the internal Variscan domain is submerged in this region. Modified of Arenas et al. (2021).

Figure 3. Zonation of the Iberian Massif showing location of the Calzadilla and Mérida ophiolites. Abbreviations: AF, Azuaga Fault; BAO, Beja-Acebuches Ophiolite; CA, Carvalhal Amphibolites; CF, Canaleja Fault; CMU, Cubito-Moura Unit; CO, Calzadilla Ophiolite; MO, Mérida Ophiolite; BCU, Badajoz-Córdoba Unit; ET, Espina Thrust; HF, Hornachos Fault; IOMZO, Internal Ossa-Morena Complex Ophiolites; LLF, Llanos Fault; MLF, Malpica-Lamego Fault; OF, Onza Fault; OVD, Obejo-Valsequillo Domain; PG-CVD, Puente Génave-Castelo de Vide Detachment; PRF, Palas de Rei Fault; PTF, Porto-Tomar Fault; RF, Riás Fault; VF, Viveiro Fault. Modified of Díez Fernández and Arenas (2015) and Arenas et al. (2016b).

Figure 4. Geological setting, general structure and lithologies of the Calzadilla (a) and Mérida (b) ophiolites. Modified of Díez Fernández et al. (2019, 2022) and Arenas et al. (2018, In press).

Figure 5. U-Pb concordia ages (zircon) of metagabbros from the Calzadilla (a) and Mérida (b) ophiolites. U-Pb zircon data recalculated after Arenas et al. (2018, In press), using the same methodology indicated in those works.

Figure 6. Whole-rock geochemical diagrams for the mafic rocks of the Calzadilla and Mérida ophiolites. a), b) Nb/Y-Zr-Ti and AFM classification diagrams, after Pearce (1996) and Irvine

and Baragar (1971), respectively. c) Chondrite-normalized REE plots (Nakamura 1974). d) TiO_2-MnO-P_2O_5 discrimination diagram (Mullen, 1983).

Figure 7. Tectonic setting discrimination diagrams for the mafic rocks. a) Nb/Y-Th/Yb diagram (Shervais 1982, Pearce 2008, 2014). b) Ti-V diagram (Shervais 1982, Pearce 2014).

Figure 8. Ti/V-Th/Nb tectonic setting discrimination diagram for the mafic rocks (Shervais 2022).

Figure 9. N-MORB-normalized immobile incompatible element patterns (Pearce 2014; normalizing N-MORB values after Sun and McDonough 1989) for average compositions of the mafic rocks of the Calzadilla and Mérida ophiolites.

Figure 10. Initial ƐHf(t) versus age diagram for zircons of Calzadilla (gabbro) and Mérida (gabbro and granite) ophiolites, showing the evolution trend of Cadomian, Mesoproterozoic, Paleoproterozoic and Archean crusts. The evolution trend of MORB (176Lu/177Hf= 0.02; Blichert-Toft and Albarède 2008) is shown, as well as the depleted mantle evolution and the chondritic uniform reservoir (CHUR). The common present-day crustal evolution trend (176Lu/177Hf = 0.0113; Taylor and McLennan 1985, Wedepohl 1995) is also shown. Isotopic Hf and U-Pb data after Arenas et al. (2018, In press).

Figure 11. a) X-Ray phase map showing the textural distribution of mineral phases in garnet amphibolite sample 117350 from the Mérida Ophiolite. b) U-Pb Tera-Wasserburg plot for garnet from sample 117350. Modified of Arenas et al. (In press).

Figure 12. Geodynamic model suggested for the generation of the Calzadilla and Mérida ophiolites and the evolution of the NW African margin of Gondwana during the interval 600-534 Ma. Modified of Arenas et al. (In press).

Figure 13. The PANALESIS plate tectonic model. Reconstruction maps showing scenarios for Cadomia evolution at (a) 600 Ma, (b) 580 Ma, (c) 560 Ma and (d) 540 Ma. The approximated location suggested for the SW Iberia Cadomian ophiolites is also shown. The time resolution of the model is 10 Myrs.

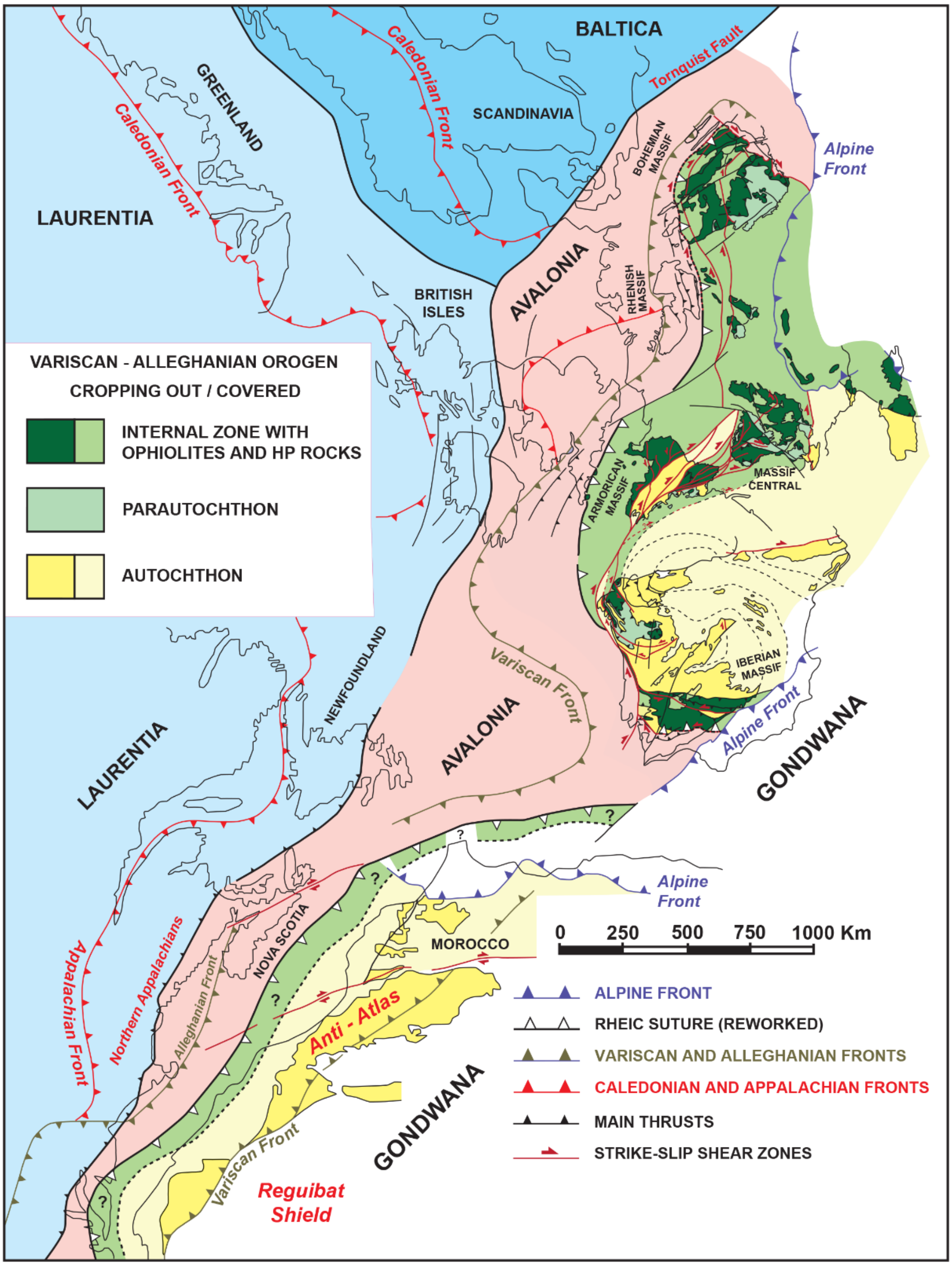
BALTICA
Caledonian Front
SCANDINAVIA
Tornquist Fault
GREENLAND
Caledonian Front
LAURENTIA
Alpine Front
BOHEMIAN MASSIF
AVALONIA
RHENISH MASSIF
BRITISH ISLES
VARISCAN - ALLEGHANIAN OROGEN
CROPPING OUT / COVERED
INTERNAL ZONE WITH OPHIOLITES AND HP ROCKS
PARAUTOCHTHON
AUTOCHTHON
ARMORICAN MASSIF
MASSIF CENTRAL
NEWFOUNDLAND
LAURENTIA
Variscan Front
AVALONIA
IBERIAN MASSIF
Alpine Front
GONDWANA
?
Alpine Front
MOROCCO
0 250 500 750 1000 Km
NOVA SCOTIA
Alleghanian Front
Northern Appalachians
Appalachian Front
Anti - Atlas
Variscan Front
GONDWANA
Reguibat Shield
ALPINE FRONT
RHEIC SUTURE (REWORKED)
VARISCAN AND ALLEGHANIAN FRONTS
CALEDONIAN AND APPALACHIAN FRONTS
MAIN THRUSTS
STRIKE-SLIP SHEAR ZONES

Figure 1

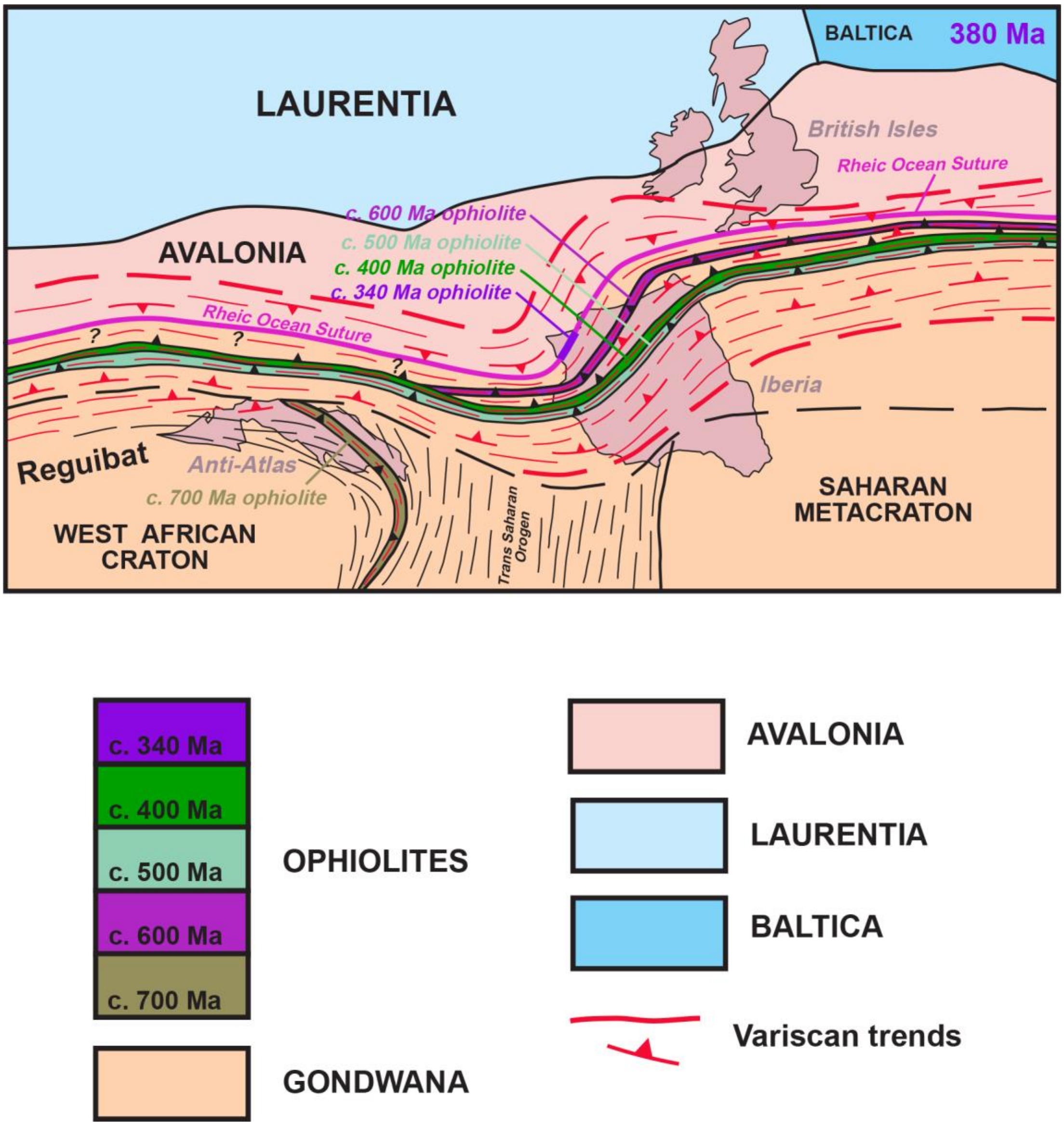
LAURENTIA
BALTICA
380 Ma
British Isles
Rheic Ocean Suture
AVALONIA
c. 600 Ma ophiolite
c. 500 Ma ophiolite
c. 400 Ma ophiolite
c. 340 Ma ophiolite
Rheic Ocean Suture
?
?
?
Iberia
Reguibat
Anti-Atlas
c. 700 Ma ophiolite
WEST AFRICAN CRATON
Trans Saharan Orogen
SAHARAN METACRATON
c. 340 Ma
c. 400 Ma
c. 500 Ma
c. 600 Ma
c. 700 Ma
OPHIOLITES
GONDWANA
AVALONIA
LAURENTIA
BALTICA
Variscan trends

Figure 2

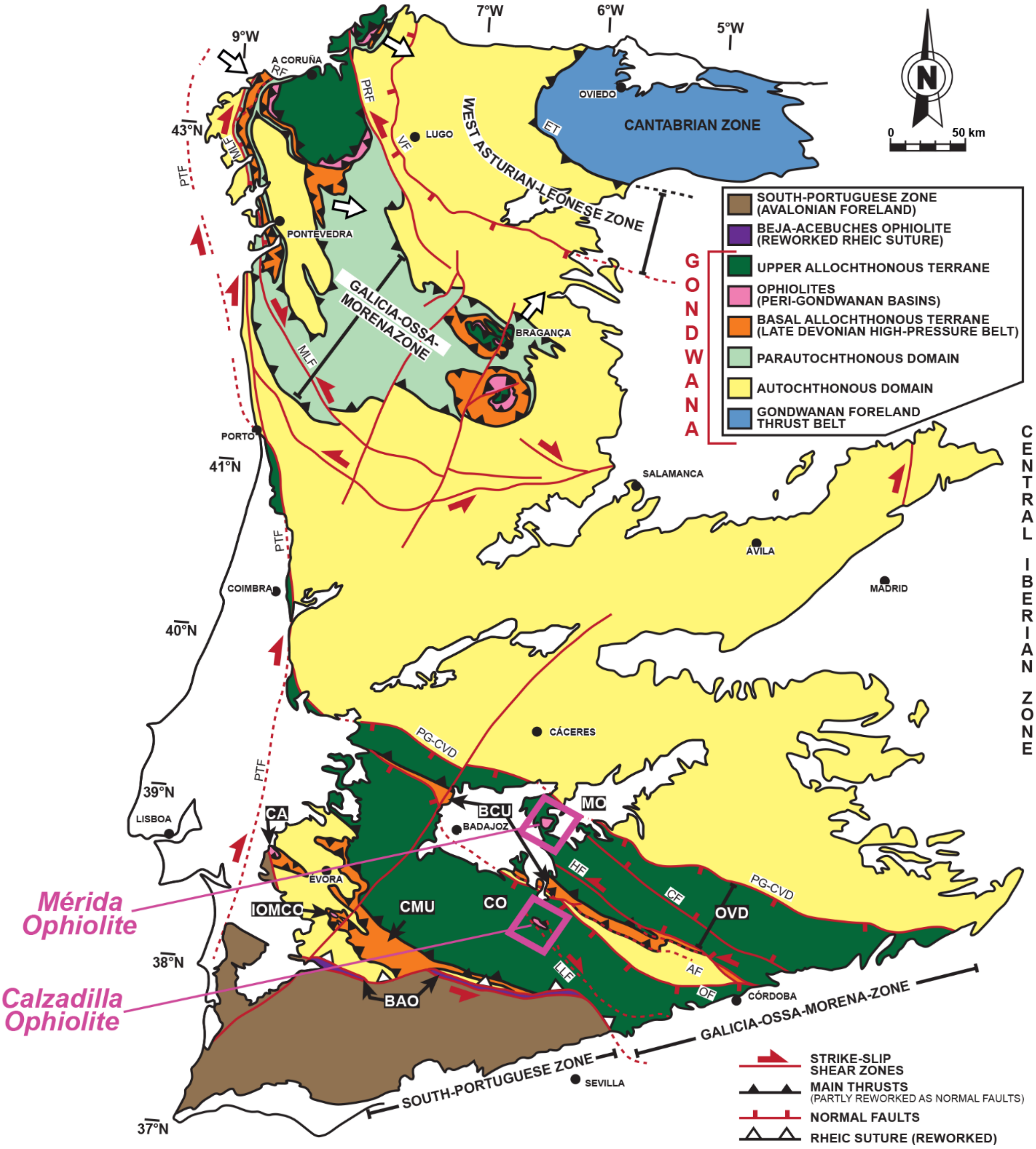
7°W
6°W
5°W
9°W
N
0
50 km
A CORUÑA
RF
MLF
PTF
43°N
PRF
VF
LUGO
OVIEDO
ET
CANTABRIAN ZONE
WEST ASTURIAN-LEONESE ZONE
PONTEVEDRA
GALICIA-OSSA-MORENA ZONE
MLF
BRAGANÇA
PORTO
41°N
SALAMANCA
PTF
ÁVILA
COIMBRA
MADRID
40°N
CÁCERES
PG-CVD
PTF
39°N
LISBOA
CA
BCU
BADAJOZ
MO
HF
CF
PG-CVD
ÉVORA
IOMCO
CMU
CO
OVD
38°N
AF
LLF
OF
BAO
CÓRDOBA
SEVILLA
37°N
Mérida Ophiolite
Calzadilla Ophiolite
GALICIA-OSSA-MORENA-ZONE
SOUTH-PORTUGUESE ZONE
CENTRAL IBERIAN ZONE
GONDWANA
SOUTH-PORTUGUESE ZONE (AVALONIAN FORELAND)
BEJA-ACEBUCHES OPHIOLITE (REWORKED RHEIC SUTURE)
UPPER ALLOCHTHONOUS TERRANE
OPHIOLITES (PERI-GONDWANAN BASINS)
BASAL ALLOCHTHONOUS TERRANE (LATE DEVONIAN HIGH-PRESSURE BELT)
PARAUTOCHTHONOUS DOMAIN
AUTOCHTHONOUS DOMAIN
GONDWANAN FORELAND THRUST BELT
STRIKE-SLIP SHEAR ZONES
MAIN THRUSTS (PARTLY REWORKED AS NORMAL FAULTS)
NORMAL FAULTS
RHEIC SUTURE (REWORKED)

Figure 3

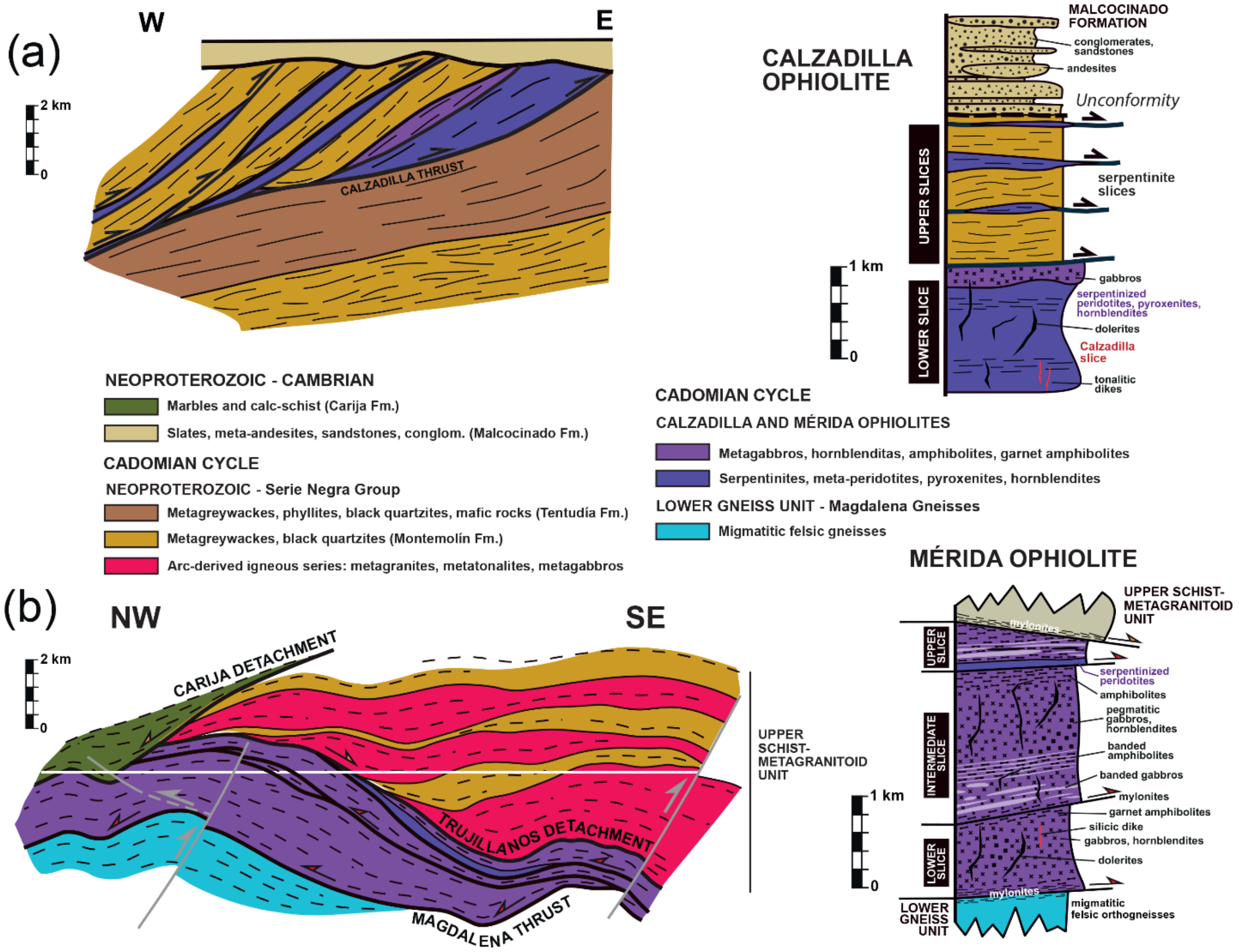
(a)
W
E
2 km
0
CALZADILLA THRUST
CALZADILLA OPHIOLITE
MALCOCINADO FORMATION
conglomerates, sandstones
andesites
Unconformity
UPPER SLICES
serpentinite slices
1 km
0
LOWER SLICE
gabbros
serpentinized peridotites, pyroxenites, hornblendites
dolerites
Calzadilla slice
tonalitic dikes
NEOPROTEROZOIC - CAMBRIAN
Marbles and calc-schist (Carija Fm.)
Slates, meta-andesites, sandstones, conglom. (Malcocinado Fm.)
CADOMIAN CYCLE
NEOPROTEROZOIC - Serie Negra Group
Metagreywackes, phyllites, black quartzites, mafic rocks (Tentudía Fm.)
Metagreywackes, black quartzites (Montemolín Fm.)
Arc-derived igneous series: metagranites, metatonalites, metagabbros
CADOMIAN CYCLE
CALZADILLA AND MÉRIDA OPHIOLITES
Metagabbros, hornblenditas, amphibolites, garnet amphibolites
Serpentinites, meta-peridotites, pyroxenites, hornblendites
LOWER GNEISS UNIT - Magdalena Gneisses
Migmatitic felsic gneisses
(b)
NW
SE
2 km
0
CARIJA DETACHMENT
TRUJILLANOS DETACHMENT
MAGDALENA THRUST
UPPER SCHIST-METAGRANITOID UNIT
MÉRIDA OPHIOLITE
UPPER SCHIST-METAGRANITOID UNIT
mylonites
UPPER SLICE
serpentinized peridotites
amphibolites
INTERMEDIATE SLICE
pegmatitic gabbros, hornblendites
banded amphibolites
banded gabbros
mylonites
1 km
0
garnet amphibolites
LOWER SLICE
silicic dike
gabbros, hornblendites
dolerites
mylonites
LOWER GNEISS UNIT
migmatitic felsic orthogneisses

Figure 4

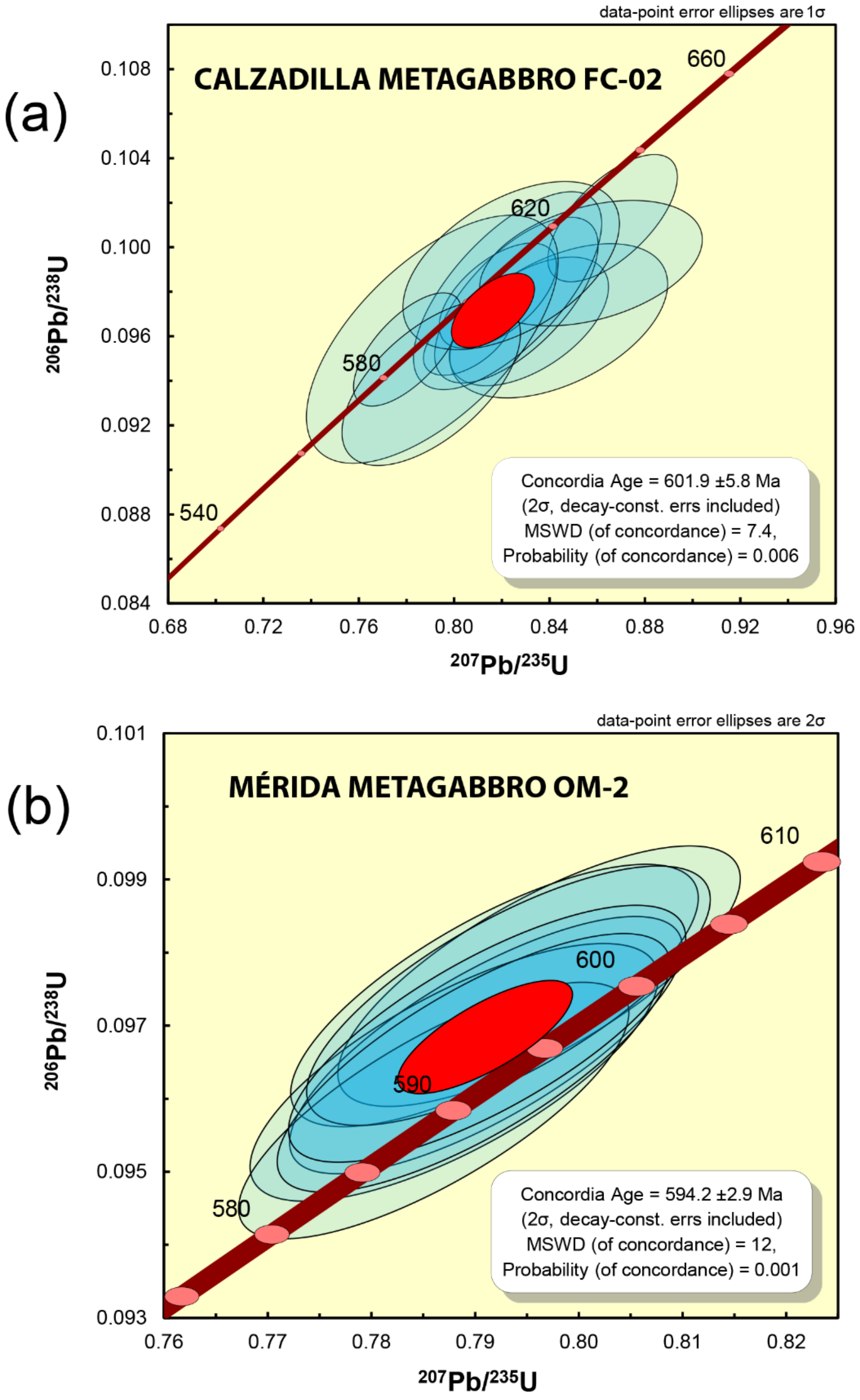
data-point error ellipses are 1σ
(a)
CALZADILLA METAGABBRO FC-02
660
620
580
540
0.108
0.104
0.100
0.096
0.092
0.088
0.084
0.68
0.72
0.76
0.80
0.84
0.88
0.92
0.96
$^{206}Pb/^{238}U$
$^{207}Pb/^{235}U$
Concordia Age = 601.9 ±5.8 Ma
(2σ, decay-const. errs included)
MSWD (of concordance) = 7.4,
Probability (of concordance) = 0.006
data-point error ellipses are 2σ
(b)
MÉRIDA METAGABBRO OM-2
610
600
590
580
0.101
0.099
0.097
0.095
0.093
0.76
0.77
0.78
0.79
0.80
0.81
0.82
$^{206}Pb/^{238}U$
$^{207}Pb/^{235}U$
Concordia Age = 594.2 ±2.9 Ma
(2σ, decay-const. errs included)
MSWD (of concordance) = 12,
Probability (of concordance) = 0.001

Figure 5

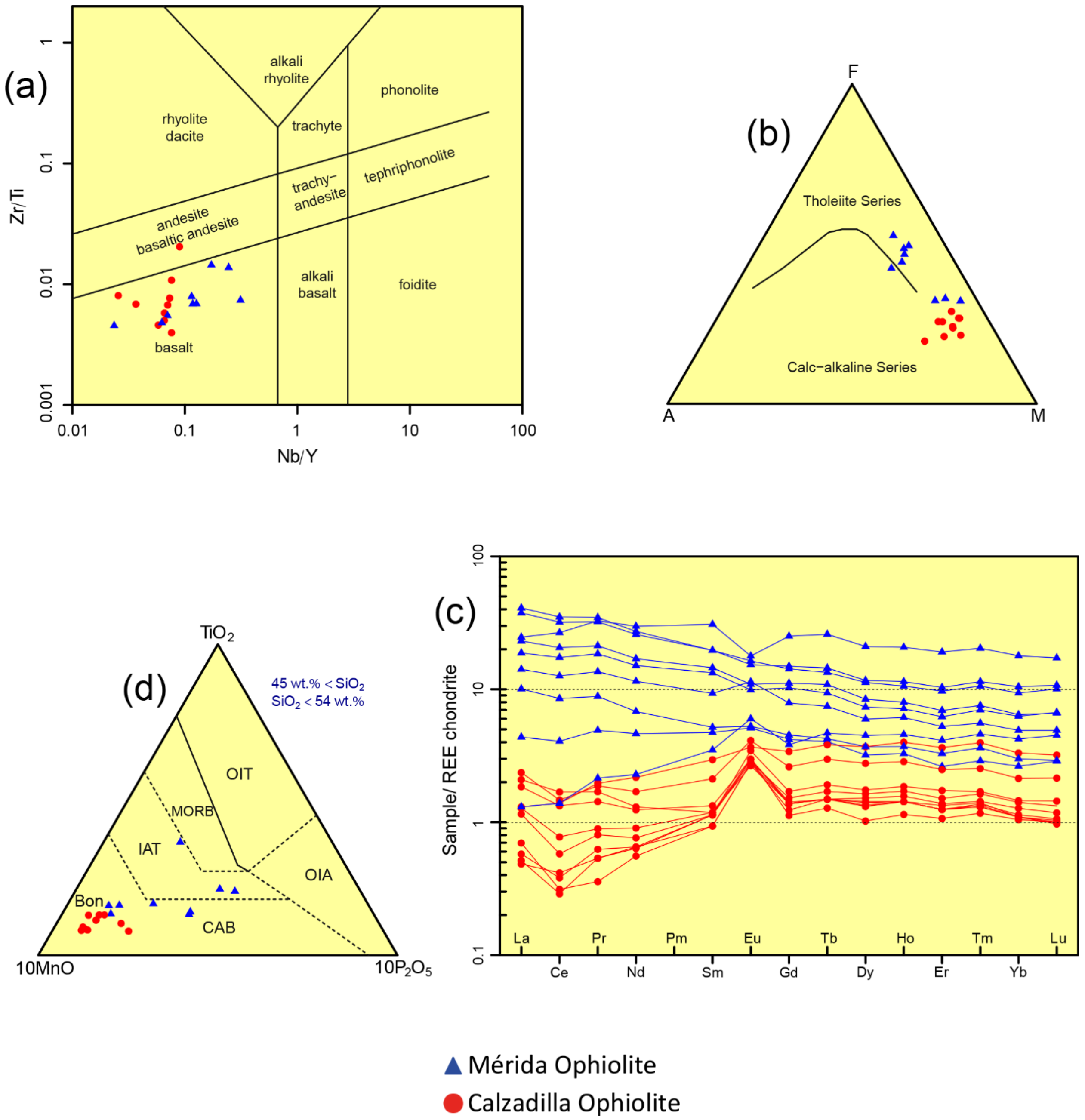
(a)
Zr/Ti
1
0.1
0.01
0.001
0.01
0.1
1
10
100
Nb/Y
alkali rhyolite
rhyolite dacite
phonolite
trachyte
tephriphonolite
trachy-andesite
andesite
basaltic andesite
alkali basalt
foidite
basalt
(b)
F
A
M
Tholeiite Series
Calc−alkaline Series
(c)
Sample/ REE chondrite
100
10
1
0.1
La
Ce
Pr
Nd
Pm
Sm
Eu
Gd
Tb
Dy
Ho
Er
Tm
Yb
Lu
(d)
TiO_2
10MnO
$10P_2O_5$
45 wt.% < SiO_2
SiO_2 < 54 wt.%
OIT
MORB
IAT
OIA
Bon
CAB
▲ Mérida Ophiolite
● Calzadilla Ophiolite

Figure 6

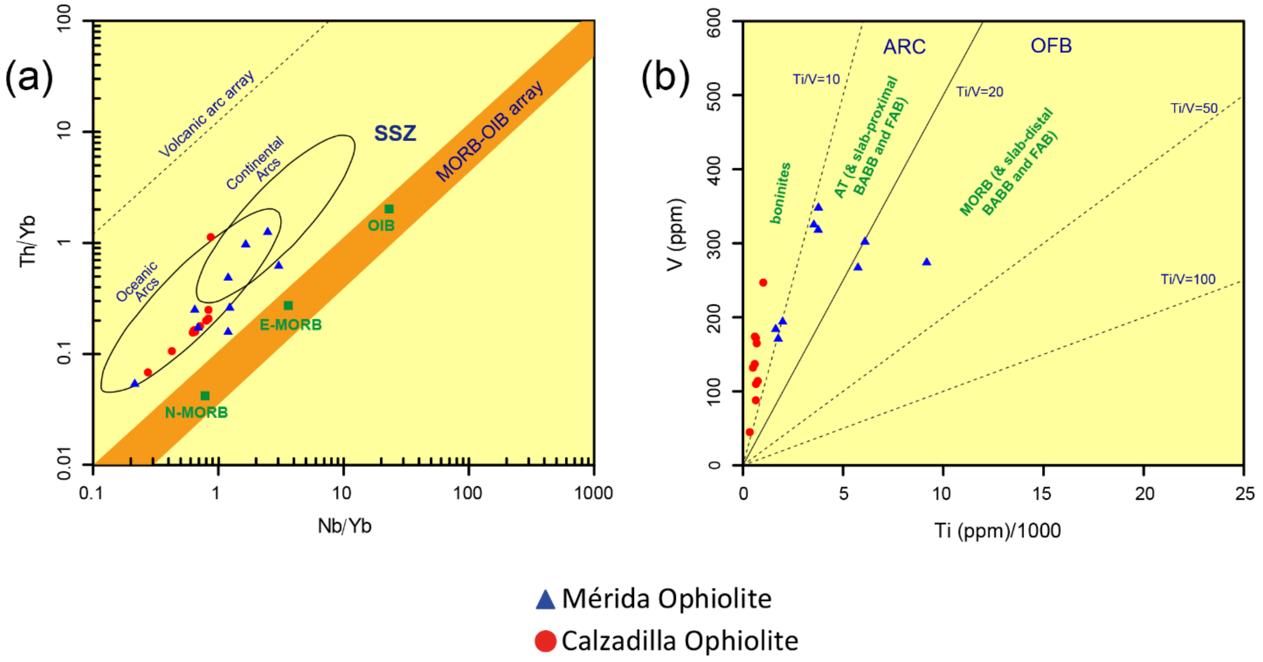
(a)
Th/Yb
Nb/Yb
100
10
1
0.1
0.01
0.1
1
10
100
1000
Volcanic arc array
Continental Arcs
Oceanic Arcs
SSZ
MORB-OIB array
OIB
E-MORB
N-MORB
(b)
V (ppm)
Ti (ppm)/1000
600
500
400
300
200
100
0
0
5
10
15
20
25
ARC
OFB
Ti/V=10
Ti/V=20
Ti/V=50
Ti/V=100
boninites
AT (& slab-proximal BABB and FAB)
MORB (& slab-distal BABB and FAB)
▲ Mérida Ophiolite
● Calzadilla Ophiolite

Figure 7

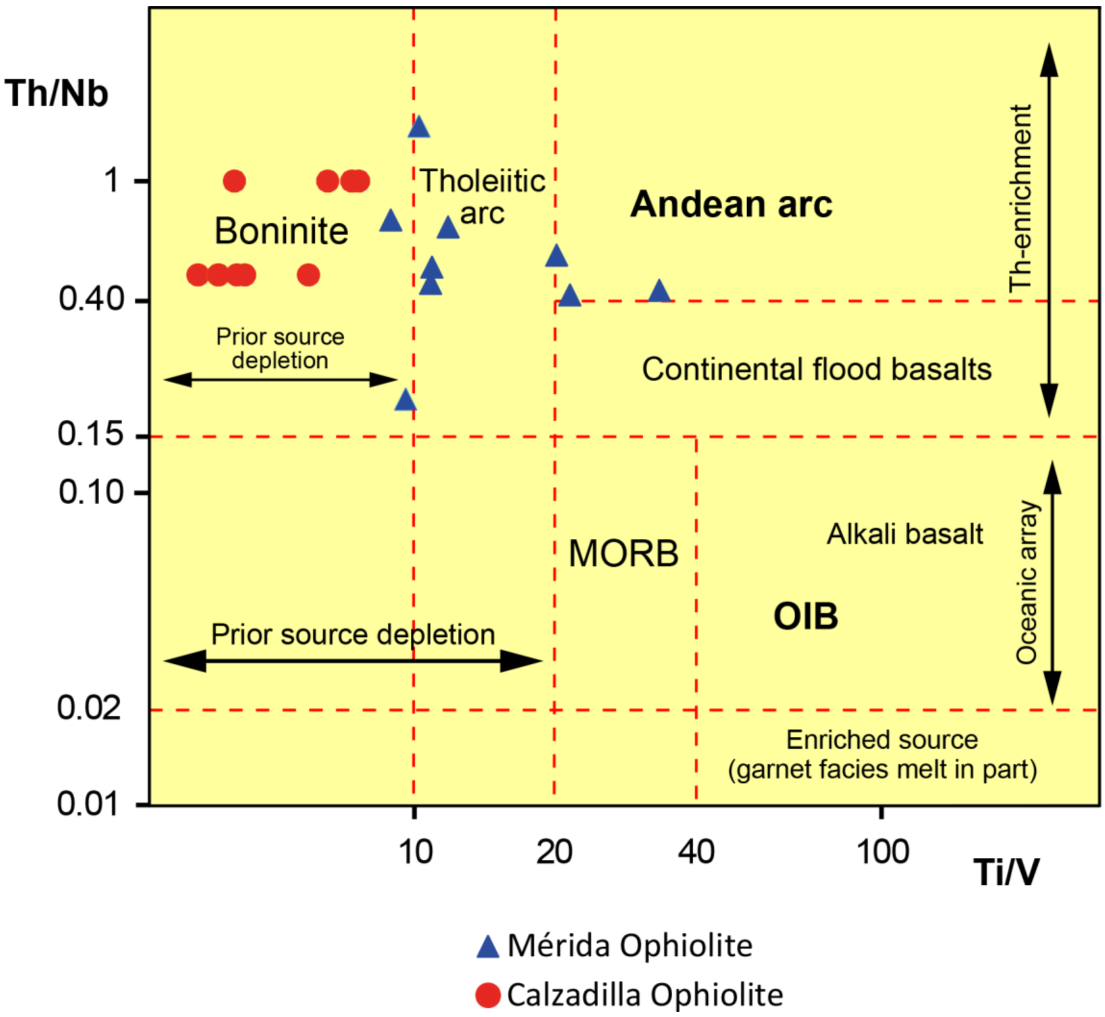
Th/Nb
1
0.40
0.15
0.10
0.02
0.01
10
20
40
100
Ti/V
Boninite
Tholeiitic arc
Andean arc
Th-enrichment
Prior source depletion
Continental flood basalts
MORB
Alkali basalt
OIB
Oceanic array
Prior source depletion
Enriched source (garnet facies melt in part)
▲ Mérida Ophiolite
● Calzadilla Ophiolite

Figure 8

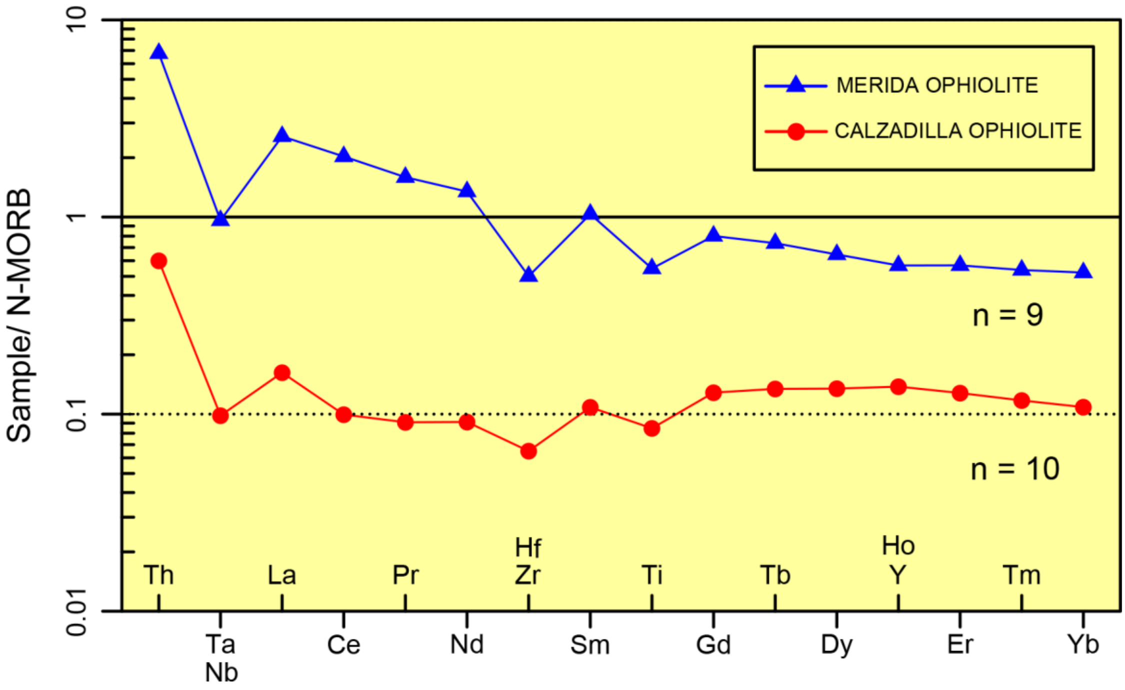

10
1
0.1
0.01
Sample/ N-MORB
MERIDA OPHIOLITE
CALZADILLA OPHIOLITE
n = 9
n = 10
Th
Ta
Nb
La
Ce
Pr
Nd
Hf
Zr
Sm
Ti
Gd
Tb
Dy
Ho
Y
Er
Tm
Yb

Figure 9

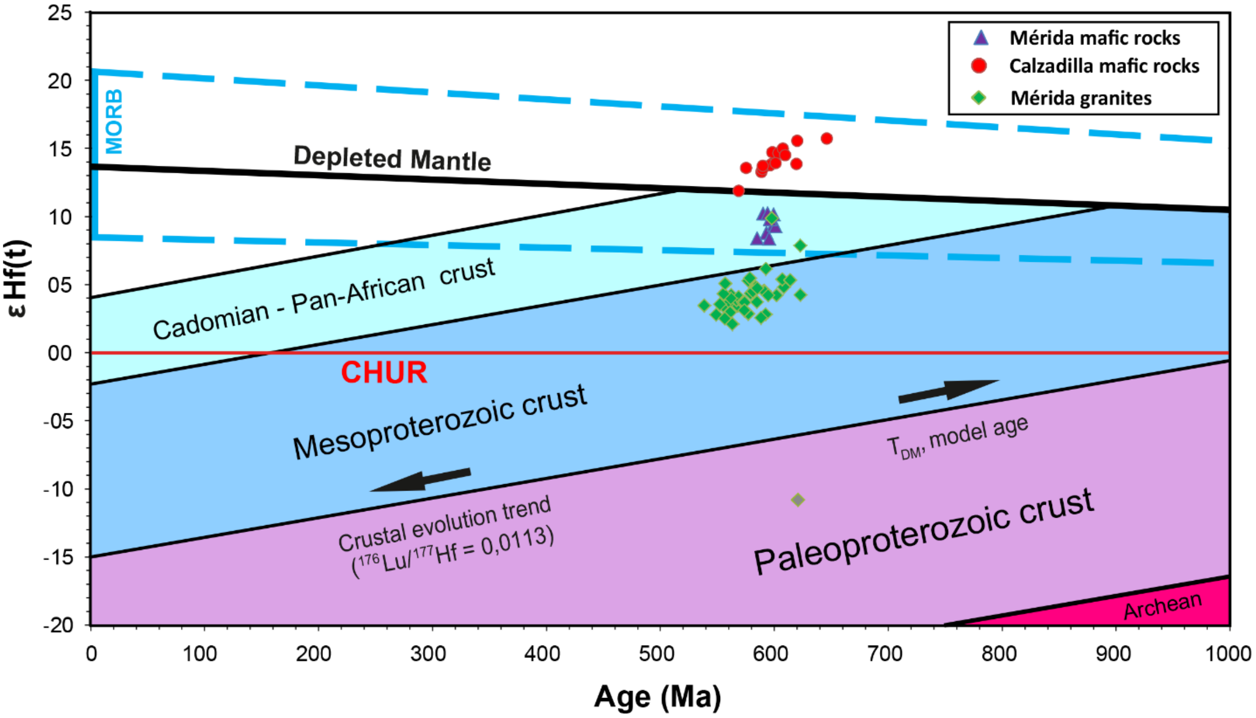

Mérida mafic rocks
Calzadilla mafic rocks
Mérida granites
MORB
Depleted Mantle
Cadomian - Pan-African crust
CHUR
Mesoproterozoic crust
Crustal evolution trend
(^{176}Lu/^{177}Hf = 0,0113)
T$_{DM}$, model age
Paleoproterozoic crust
Archean
εHf(t)
25
20
15
10
05
00
-05
-10
-15
-20
0
100
200
300
400
500
600
700
800
900
1000
Age (Ma)

Figure 10

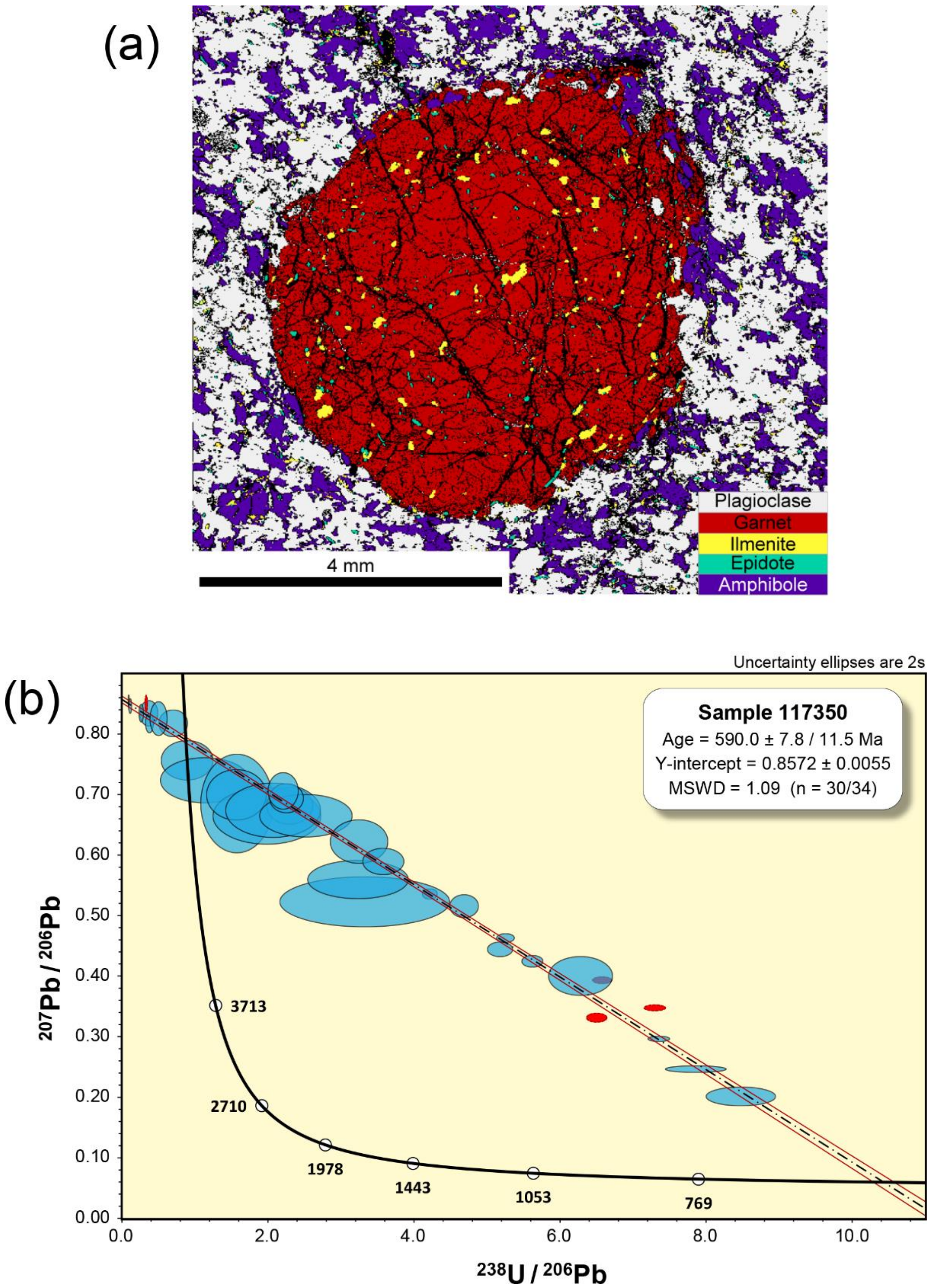
(a)
Plagioclase
Garnet
Ilmenite
Epidote
Amphibole
4 mm
(b)
Uncertainty ellipses are 2s
Sample 117350
Age = 590.0 ± 7.8 / 11.5 Ma
Y-intercept = 0.8572 ± 0.0055
MSWD = 1.09 (n = 30/34)
3713
2710
1978
1443
1053
769
0.00
0.10
0.20
0.30
0.40
0.50
0.60
0.70
0.80
0.0
2.0
4.0
6.0
8.0
10.0
207Pb / 206Pb
238U / 206Pb

Figure 11

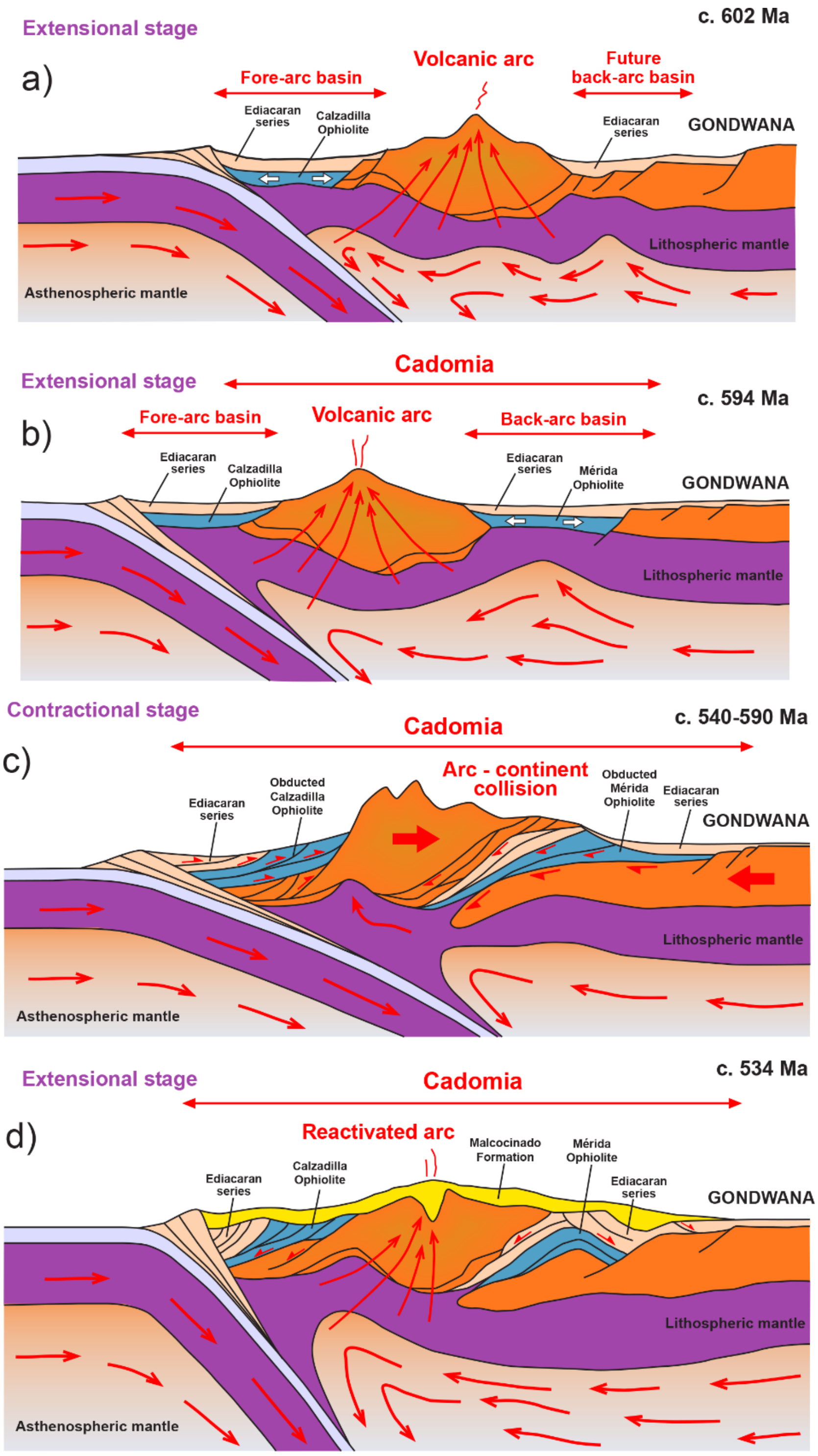
Extensional stage
c. 602 Ma
a)
Volcanic arc
Fore-arc basin
Future back-arc basin
Ediacaran series
Calzadilla Ophiolite
Ediacaran series
GONDWANA
Lithospheric mantle
Asthenospheric mantle
Extensional stage
Cadomia
c. 594 Ma
b)
Fore-arc basin
Volcanic arc
Back-arc basin
Ediacaran series
Calzadilla Ophiolite
Ediacaran series
Mérida Ophiolite
GONDWANA
Lithospheric mantle
Contractional stage
Cadomia
c. 540-590 Ma
c)
Arc - continent collision
Obducted Calzadilla Ophiolite
Ediacaran series
Obducted Mérida Ophiolite
Ediacaran series
GONDWANA
Lithospheric mantle
Asthenospheric mantle
Extensional stage
Cadomia
c. 534 Ma
d)
Reactivated arc
Malcocinado Formation
Mérida Ophiolite
Calzadilla Ophiolite
Ediacaran series
Ediacaran series
GONDWANA
Lithospheric mantle
Asthenospheric mantle

Figure 12

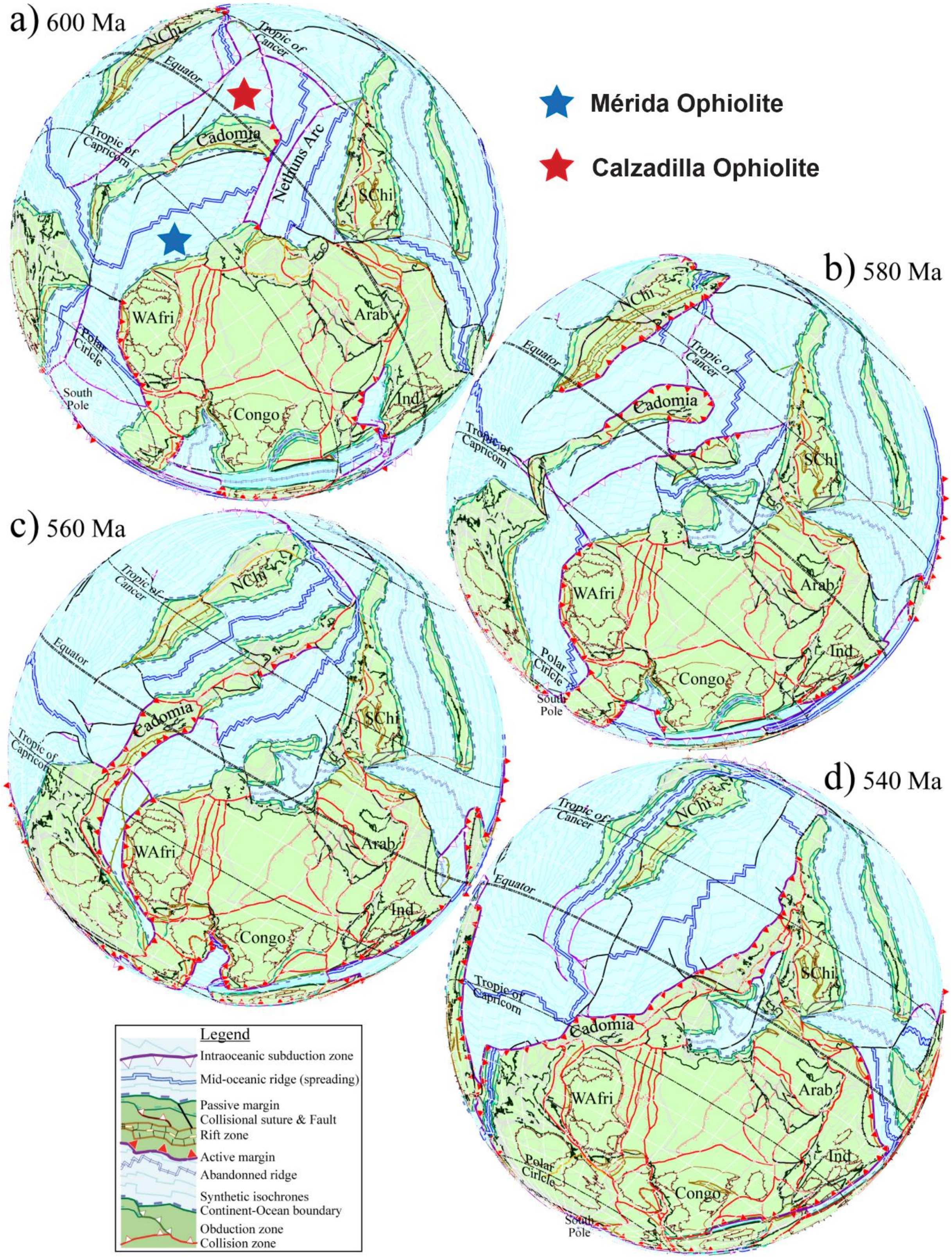
a) 600 Ma
Mérida Ophiolite
Calzadilla Ophiolite
NChi
Equator
Tropic of Cancer
Tropic of Capricorn
Cadomia
Nethuns Arc
SChi
WAfri
Arab
Polar Circle
South Pole
Congo
Ind
b) 580 Ma
NChi
Equator
Tropic of Cancer
Cadomia
Tropic of Capricorn
SChi
WAfri
Arab
Polar Circle
South Pole
Ind
Congo
c) 560 Ma
Tropic of Cancer
NChi
Equator
Cadomia
SChi
Tropic of Capricorn
WAfri
Arab
Ind
Congo
d) 540 Ma
Tropic of Cancer
NChi
Equator
Tropic of Capricorn
Cadomia
SChi
WAfri
Arab
Polar Circle
Ind
Congo
South Pole
Legend
Intraoceanic subduction zone
Mid-oceanic ridge (spreading)
Passive margin
Collisional suture & Fault
Rift zone
Active margin
Abandonned ridge
Synthetic isochrones
Continent-Ocean boundary
Obduction zone
Collision zone

Figure 13